T H E U N I V E R S I T Y O F M I C H I G A N

Final Report

Analysis of Micrometeorological and Related Data obtained at the U. S. Army SIPRE Keweenaw Field Station Houghton, Michigan

Part II

Data Processing and Analysis

Part III

Participation in Data Collection Program

Donald J. Portman
Associate Research Meteorologist

Edward Ryznar
Graduate Research Assistant

UMRI Project 02688

Under Contract With:

U. S. Army Snow, Ice and Permafrost Research Establishment
Corps of Engineers
1215 Washington Avenue
Wilmette, Illinois

Administered by:

THE UNIVERSITY OF MICHIGAN RESEARCH INSTITUTE ANN ARBOR

May 1960

PREFACE

The work described in this report was conducted under U. S. Army Snow, Ice and Permafrost Research Establishment, Corps of Engineers, Contract DA-11-190-ENG-30. The general purpose was to evaluate heat transfer processes between a snow cover and its environment in order to predict physical snow cover characteristics.

Work on the contract included (1) processing, tabulation, and analysis of data collected during the 1954-55 and 1955-56 snow seasons at the Keweenaw Field Station, Houghton, Michigan and (2) participation in the data collection program for the 1957-58 and 1958-59 snow seasons.

The processed and tabulated thermal radiation data for the 1954-55 and 1955-56 snow seasons are given in Part I of the Final Report, dated January, 1960. Part II presents the results of the analysis phase of the work and Part III a brief resume of participation in the data collection program. A group of graphs prepared as part of the processing phase is submitted under separate cover.

The authors wish to express their appreciation to Mr. Dwight Meeks for his assistance in the measurement phase of the investigation, (Mrs.) Ruth Baehr and (Mrs.) Ruth Hayes for their work in data processing, and to (Mrs.) Joy Beil for typing the Final Report.

TABLE OF CONTENTS

LIST OF TABLES

LIST OF FIGURES

ABSTRACT

The heat exchange of a snow cover was studied with respect to (1) the effects of heat transfer processes on metamorphic action within the snow cover and (2) the prediction of heat fluxes and the resulting changes in snow cover characteristics from standard meteorological information. The variables and processes in the earth-snow-atmosphere system and their inter-relationships are defined and discussed in terms of the thermal interaction between a snow cover and its environment.

Data collected at the U. S. Army, S. I. P. R. E., Keweenaw Field Station, Houghton, Michigan, were used to determine heat transfer by thermal radiation, convection, and conduction. The direct dependence of incident solar radiation, atmospheric radiation and net radiation on different types and amounts of cloud cover is shown. The Liljequist method for computing turbulent heat transfer and conduction heat transfer in snow was used. The dependence of low-level inversions and turbulent heat transfer on cloudiness and wind speed is shown. Average air temperature is shown to exert a pronounced effect upon snow heat conduction, cold content, and temperature profile.

The influence of the snow temperature profile on the physical characteristics of snow and the possible application of this information to engineering problems are discussed.

PART II

DATA PROCESSING AND ANALYSIS

A. INTRODUCTION

Physical characteristics of a snow cover undergo continual change in direct response to changing meteorological conditions. The meteorological influences, analagous to weathering in geological processes, combine with influences of the earth beneath the snow cover to form an environment responsible for a snow metamorphism capable of causing changes in physical properties that may be extremely significant for various engineering activities. Except for precipitation, all meteorological influences may be regarded as effects of the transfer of momentum, heat and water vapor between the atmosphere and the snow cover. The effects of momentum transfer, in even a light wind, are plainly evident to a casual observer and can seldom be neglected in a complete accounting of snow metamorphic processes. The transfers of heat and water vapor, on the other hand, are inherently more subtle. In the absence of melting, their effects may slowly accumulate and amount to a complete transformation of the snow cover in a period of several days or weeks. Complete understanding of the meteorological influences on the metamorphism of a snow cover must depend on a detailed measurement and analysis of the above-mentioned transfer processes. Significant analysis is highly dependent, furthermore, on accurate measurement of many variables in and near a natural snow cover.

The development of a measurement system at the Keweenaw Field Station represents a unique attempt to obtain all information required for a complete analysis of the meteorological and sub-surface influences on snow-cover metamorphism. The data from this station for two winter seasons were selected for processing and selective analysis in order to explore various relationships in the heat transfer components of the metamorphic processes and to evaluate the adequacy of the measurement system. Heat transfer was selected in favor of the other processes mainly because of its first-order influence on snow properties of engineering interest and because of its significance in the momentum and water vapor transfer mechanisms.

Quantitative analysis of the individual heat transfer components would be meaningless for understanding or estimating metamorphic processes without a synthesis of their interactions and combined effects on the snow cover. For this purpose the temperature structure within the snow cover serves as a logical product of heat transfer processes and a natural reference for understanding the transformations within the snow cover comprising its metamorphism. In the following section the various components of heat transfer involved in determining the temperature distribution in a snow cover are discussed with respect to their interactions and dependence on meteorological and sub-surface conditions.

B. ESTIMATING SNOW TEMPERATURE DISTRIBUTIONS FROM METEOROLOGICAL INFORMATION

The vertical temperature distribution in a snow cover at a given time may be regarded as the result of (1) the history of heat gains and losses and (2) the thermal properties of the snow. Since the thermal properties of the snow are themselves dependent upon the thermal history of the snow cover, it should be possible to specify the snow temperature distribution in terms of heat transfer to and from the snow cover. For estimating snow temperature distributions, and hence various snow physical properties in remote areas, it is reasonable to expect some success by estimating heat transfer from standard meteorological data and terrain information. Because of the time required for snow to change characteristics in response to internal temperature distributions, this approach to predicting snow conditions depends more on a knowledge of past weather conditions than on a prediction of future conditions. It can be imagined that from a continuous knowledge of atmospheric conditions for a given place, the derived physical properties of the snow cover could be logged on a daily basis.

Two separate approaches may be distinguished for utilizing meteorological information to estimate snow temperature distributions. One method would be to relate standard meteorological data (air temperature, wind speed, cloudiness, etc.,) directly to observed snow temperature distributions. If a sufficient number of observations could be obtained for a wide variety of conditions, relationships between efficient arrangements of variables could then lead to numerical expressions for general prediction purposes. Because of the wide ranges of meteorological variables in different climatic regions and because of their occurrence in many different combinations for varying time intervals, this approach may never yield an accuracy suitable for engineering application.

The second approach involves determining the amount of heat transferred by the different physical processes (conduction, convection and radiation) from knowledge of the process mechanisms The use of basic physical processes obviates the necessity to derive empirical relationships, required for the first approach, for the very many combinations of variables possible in the different climatic regions. Its weakness lies, however, largely in two distinct areas: (1) lack of understanding of the physical processes and (2) interaction among the several processes necessitating extremely complex and unwieldy analytical expressions for practical application.

Between the two extremes represented by the two approaches are various combinations involving both empirical relationships and analytical expressions for known physical processes. Figure 1 is a display of variables, processes and their inter-relationships in the earth-snow-atmosphere system. The diagram illustrates the difference between the separate approaches discussed above and aids in understanding the complex thermal interaction between a snow cover and its environment. The entire system may be viewed as a machine that runs continuously. The time-changing variables listed in the far left column are the basic input; the box on the right containing the vertical temperature distribution in snow and the resulting physical properties are the product or output.

Between the input and the output categories are the various components involved in the heat transfer processes. In the upper left-hand section are the components of the radiant heat transfer processes and in the lower left-hand section the turbulent (convective) transfer components. In the right-hand portion of the diagram are the components of the internal heat transfer processes. The temperature of the snow-atmosphere interface serves as a dependent variable

responsive to all three processes, adjusting to a temperature at any one time in accordance with the basic law of conservation of energy.

The non-thermal effects of wind and humidity are indicated by dashed lines. These input variables influence the thermal characteristics of the snow cover through mass and momentum transfer. Specifically, the snow surface characteristics, i.e., albedo, long-wave reflectivity, long-wave emissivity and aerodynamic roughness are directly influenced both by action of the wind and by moisture transfer to and from the snow crystals. There are, in addition, important direct influences of wind and humidity on the mechanical properties of the snow cover. The fact that these influences are shown as dashed lines does not imply insignificance but merely that they were not included specifically in the study of thermal processes.

For the sake of simplicity, various other complex processes are not represented in this diagram. Among those omitted are gaseous diffusion and mass transfer in the soil, penetration of solar radiation and variations of albedo due to accumulation and concentration of debris.

The input variables consist of three basic types: (1) four items completely determined by location and primarily significant for specifying solar radiation; (2) six variables determined from synoptic scale weather data and significant for both radiative and turbulent transfer processes; and, finally, (3) one variable (ground temperature) determined from meteorological information prior to the accumulation of snow and adjusted according to estimated seasonal changes (which may be based on accumulated day-to-day heat transfer effects).

The six variables in the second category may be classified as (a) upper-atmosphere information (cloudiness, and atmospheric humidity and temperature) which contribute directly to both solar (short-wave) and atmospheric (long-wave) radiation fluxes and (b) surface weather data which are directly related to the transfer of heat, water vapor, and momentum. Cloudiness, temperature, wind and dewpoint data are standard items reported at most weather stations while the humidity and temperature in the upper atmosphere are obtainable directly only from soundings. For areas in which there is not an adequate number of upper air sounding stations such data may be obtained from continental scale upper air charts with sufficient accuracy for atmospheric radiation computations.

The solar and atmospheric radiation components of the external heat transfer processes may be determined from the input variables as indicated in the upper left-hand portion of the diagram (Fig. 1). Except for their dependence on cloudiness, these components may be fairly accurately estimated from the variables listed, i.e., functional relationships, or approximations for them, are known. Gerdel, Diamond and Walsh (1) have, for example, prepared nomographs from which values of solar radiation on a daily basis may be estimated. For more detailed computation of solar radiation, the work of Klein (2) may be consulted. Atmospheric radiation for cloudless conditions may be computed with considerable accuracy following the models developed by Elsasser (3), or Brooks (4).

Combined with the solar radiation reflected from the snow surface and the long wave radiation emitted by the snow, the incident solar and atmospheric radiation components form, finally, a net radiation term. The relationships among these components are shown in the upper, central part of the diagram. The snow surface properties--temperature, albedo, long-wave reflectivity and long wave emissivity--required to compute the net radiation cannot be determined independently and must be regarded as steps in a feed-back loop required to specify net radiation. Relationships between albedo and various characteristics

of the snow cover are not well understood but may be determined from relationships involving temperature, compaction processes, etc. (See Reference 5). Long wave emissivity and reflectivity probably do not vary significantly for first approximation to system processes and may be regarded as nearly 1.0 and zero, respectively (Reference 5). The snow radiation, then, is determined from Stefan's law applied to the snow surface temperature.

Fortunately, the radiation components represented in the diagram can be measured on a continuous basis with considerable accuracy. Continental-scale measurement networks have not yet been established so that determination of the radiation components must be estimated for remote areas. In addition to snow surface temperature, a derived quantity, the most serious gaps in knowledge preventing accurate estimation of the net radiation are (1) relationships between cloudiness and incident solar and atmospheric radiation and (2) dependence of albedo on directly derivable snow properties. In processing and analyzing the Keweenaw Field Station data it was found possible to isolate information showing the direct dependence, not only of solar and atmospheric radiation, but also of net radiation, on different types and amounts of cloud cover.

The turbulent transfer components and processes unfortunately can neither be measured nor estimated with an accuracy comparable to that for the radiation components. Knowledge of turbulent mechanisms, however, appears to be advancing at an accelerating rate and it is perhaps not too optimistic to expect practical functional relations for computing heat and water vapor transfer in the not too distant future.

With regard to practical applications to the transfer of heat and water vapor from a snow surface the state-of-the-art rests largely with the long be-labored exchange coefficient hypothesis and, specifically, with relationships between the transfer coefficients for heat, mass and momentum. The problem is intimately related to the question of the dependence of the momentum transfer coefficient, i.e., the eddy diffusivity, on density stratification in the surface layer of the atmosphere. The work of Monin and Obukhov in 1954 (6) is a notable attempt to formulate a coherent theory to account for observed effects of density stratification on eddy diffusivity. Their formulation leads to equations useful for computing both heat and water vapor transfer (Sheppard 7), when the density stratification is not great, that is to say, when the conditions are near adiabatic. Much of the time, however, in many regions the air layers over snow covers exhibit strong density stratification with the coldest air adjacent to the snow, a situation that inhibits vertical motion and, thereby, heat transfer. In spite of many attempts to develop practical equations for computing turbulent heat transfer for this condition there appear to be no proven relationships. The well-known work of Sverdrup (8) should be mentioned as an early attempt to solve this problem. The most recent comparable work on the subject is that of Liljequist (9) (10) who developed a simplified equation for computing heat transfer based on a long series of observations made in the Antarctic.

Both the Monin and Obukhov and the Liljequist models were used to compute turbulent heat transfer for Keweenaw Field Station data from selected periods. The results clearly show the limitation of the Monin and Obukhov model for conditions far from adiabatic. The results obtained with the Liljequist model, on the other hand, appear to be acceptable for a wide range of stable conditions.

Heat transfer to the snow cover from the ground beneath it is represented by a heat conduction component shown in the block at the lower center part of

the diagram, Figure 1. Following the accumulation of snow on warm ground in sufficient amount to protect the latter from diurnal temperature changes, there is a small and slowly decreasing flux of heat from ground to snow. If the ground is saturated, or nearly so, the diffusion of vapor is negligible and the conduction process is the only one of significance. It is possible, therefore, to estimate this component directly from estimates of conductivity and temperature gradient. The complicating effects of diurnal changes so important to estimate radiative and turbulent convective heat transfer components are entirely absent here.

Because thermal conductivity data were not available for the analysis of the Keweenaw Field Station data it was not possible to make direct computations of soil heat flux. Daily amounts can be estimated from the soil temperature data, however, by estimating appropriate values of thermal conductivity. For this purpose a table was prepared giving daily amounts of conduction heat transfer in terms of mean temperature gradient and several suggested values of thermal conductivity.

The right side of Figure 1 shows the components and relationships of the complex heat and vapor transfer processes at work within the snow cover. Significant to the external heat transfer processes is the fact that the snow surface temperature is partly controlled by the internal conduction transfer and heat involved in change of phase resulting from water vapor migration. Since vapor migration is directly dependent upon vapor pressure gradient and since it, in turn, is largely a function of the temperature gradient, the latter becomes the most significant single controller of conditions in the snow cover.

Since the thermal conductivity of snow is small, the lower part of the snow cover does not experience the diurnal variations created by the continually varying radiative and convective heat transfer components. This part of the snow cover is therefore similar to the ground beneath it with respect to a steady heat flux independent of time of day. Thus, steady state equations may be used although the coefficients must be modified as vapor transfer effects become significant.

The properties of the snow cover important for heat and mass diffusion, i.e., thermal conductivity and porosity, are closely related to physical properties such as density, hardness, and shear strength used for characterizing the trafficability of the snow. These are the properties whose slow changes under the influence of the temperature gradient constitute the metamorphic processes of importance for engineering problems.

The many unknown functional relationships in the various processes depicted in Figure 1 are serious detriments to the application of this approach to estimating snow conditions from meteorological information. Perhaps an equally significant characteristic of the total thermal system is the large number of interrelated processes and properties. No one direct component can be separated from the others. Simulation by electrical analogue computer would appear to offer an important advantage in handling the problem since the significance of any component or the adequacy of a given formulation for a functional relationship could be readily understood. Until the entire thermal system can be depicted by such techniques the significance of research on any particular detail or aspect will be difficult to evaluate. Halstead, et.al. (11) described the advantages of electronic computer simulation in handling a problem involving heat and water vapor transfer over a grass-covered field. Following this pioneer work the U. S. Army Signal Corps Meteorology Department at Fort Huachuca contracted for the design and construction of an elaborate analogue computer which

would be admirably suited to simulate the problem of snow metamorphism. Reference may be made also to Poppendiek and Tribus (12), Merryman and Clayton (13), and Clayton, et al. (14). Hopefully, further computer development and application will be directed toward this important problem coincident with a study of the heat transfer mechanisms themselves In this way, it is probable that a complete and accurate system for estimating mechanical properties of snow from meteorological information will soon be evolved. The system must necessarily be built on a model similar to that depicted in Figure 1.

Fig. 1. HEAT TRANSFER COMPONENTS AND RELATIONSHIPS

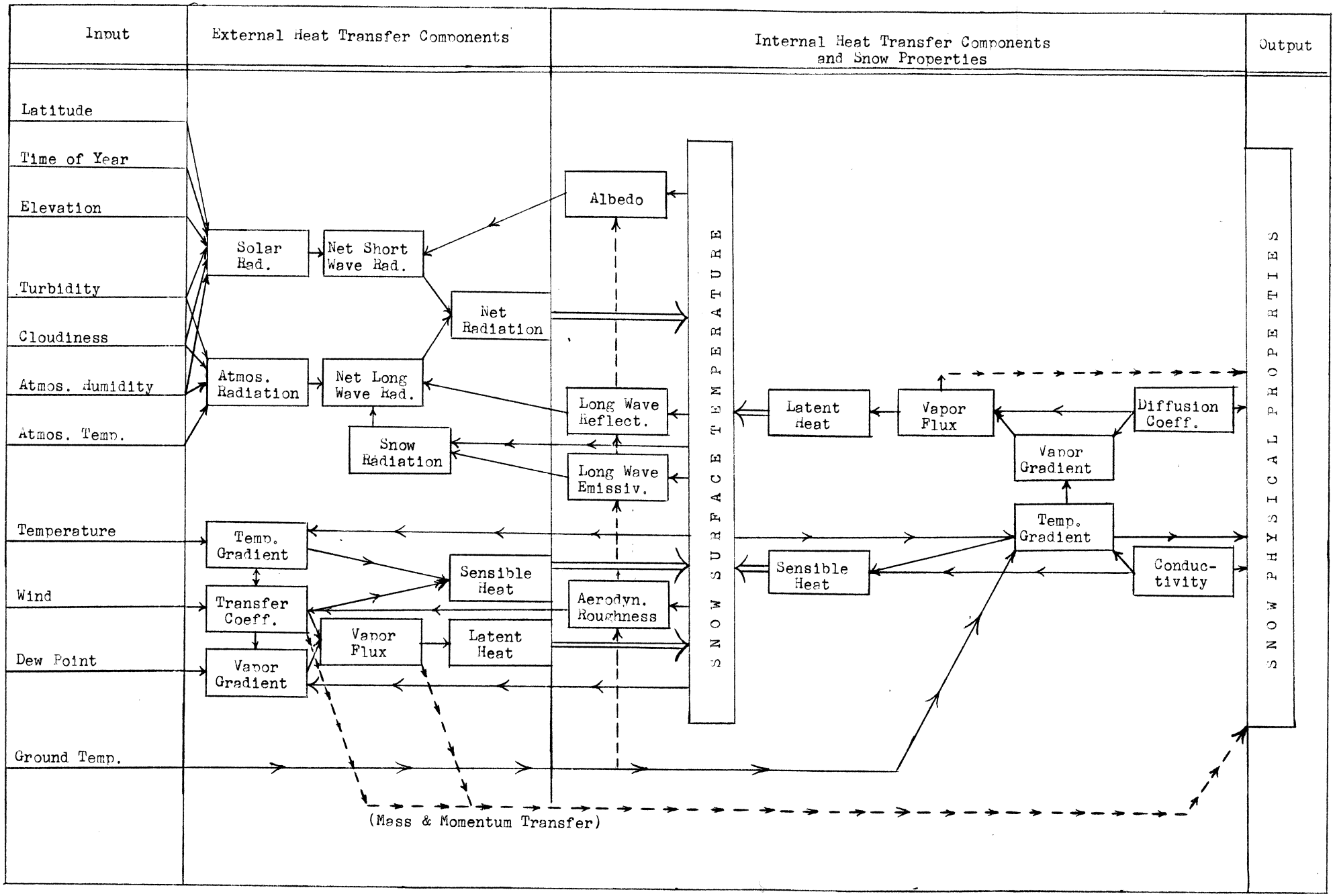

C. RADIATIVE HEAT TRANSFER

Thermal radiative fluxes depend partly on the position of the sun (time of day and season of year), partly on snow properties (reflectivity, temperature, and emissivity), and partly on meteorological conditions (atmospheric temperature, water vapor content, turbidity and cloudiness) (See Figure 1). Together, they determine the radiation exchange which plays a major part in the thermal regime of a snow cover. If the snow surface is considered as a dividing plane between the media air and snow, one part of the radiation incident on the surface is reflected into the first medium and the other part penetrates the second. The penetrating radiation is partly absorbed and partly transmitted through the uppermost snow layer. The relative amounts of energy reflected, absorbed and transmitted depend not only upon the physical conditions of individual snow layers, but also upon the wave length of the incoming energy. Thus, the components of the radiation balance vary not only in magnitude but also in ability to promulgate snow metamorphism.

Analysis of the radiation data was directed toward (1) evaluating the relative importance of the radiative fluxes as they influence snow metamorphism and (2) investigating the feasibility of predicting these fluxes given hourly weather observations reported by an FAA weather station adjacent to the Keweenaw Field Station. Reference is made to Part I of this report for a description of the instrumentation used in the radiation measurements and a tabulation of all radiation data collected.

1. SHORT-WAVE RADIATION

a) Incident Solar

Of the several components which comprise the radiation balance over snow, the radiation energy of sun (direct plus diffuse) is the largest. Ninety-nine per cent of the solar, i.e., short-wave, radiation is between 0.15 microns and 4 microns in the electromagnetic spectrum. Its maximum intensity is in the visible spectrum at about 0.5 microns. The daily amount of solar radiation incident on a horizontal surface at the outer limit of the earth's atmosphere may be calculated from the solar constant for any given latitude and time of year as a function of the angle of incidence of the sun's rays, the duration of sunlight, and the distance between earth and sun.

Some of the incident solar radiation is reflected and scattered by air molecules and particles and some is absorbed by water vapor and other substances in the atmosphere. By far, the largest variations in the portion of solar radiation transmitted by the atmosphere are caused by clouds. The type, height, density, thickness and amount of clouds are important in determining the amount of solar radiation which reaches the snow. Several investigators have related the ratio of incoming solar radiation measured at the earth's surface to that received at the earth's surface with cloudless skies, to the amount of cloud cover (15). An inherent difficulty in these investigations has been the considerable variation in this value from season to season, location to location, and for various cloud types, densities, and thicknesses. However, at one location for a single season it is reasonable to expect that a useful relationship might be derived for predicting solar radiation from cloud information. Since solar radiation reflected by snow is proportional to that which is incident, it follows a similar pattern in its dependence on cloudiness.

Effects of Cloudiness - The dependence of measured solar radiation upon cloud conditions was studied using the daily totals (ly/day) obtained at the Keweenaw Field Station for approximately 130 days in January, February, and March, 1955 and 1956. The ratio of each daily total of measured solar radiation to the daily total reaching the outer limit of the earth's atmosphere was computed. The latter quantities were interpolated from a curve of solar radiation versus latitude given in Reference 16. The resulting percentages were related to cloudiness categorized according to average morning and afternoon heights and amounts. The results are listed in Table 1. The table shows, for example, that an average of 60-70% of the total daily insolation at the outer limit of the atmosphere reached the snow cover when the following cloudiness occurred: (1) an overcast higher than 5000 feet all day, or (2) an overcast lower than 3000 feet in the morning (or afternoon) and broken clouds lower than 3000 feet in the afternoon (or morning). Percentages of measured solar radiation ranged from 94 with a clear day in March to 17 with a partially obscured low overcast and freezing drizzle. The data during precipitation conditions with nearly calm winds were inaccurate because of the tendency for snow or ice to accumulate on the pyrheliometer.

A second relationship between measured solar radiation, cloudiness and time of day is shown in Figure 2. The analysis was made by (1) grouping hourly cloud observations in height and amount categories, (2) grouping hourly totals of measured solar radiation into each category and (3) averaging all hourly totals within each cloudiness category. Arbitrary adjustments were necessary because of relatively few samples in certain cloudiness categories, but in general, it is thought that dependence of the incident short-wave radiation is well defined. The diurnal patterns, representing the last two weeks in January and the entire month of February, show solar radiation as a function of cloudiness at the Keweenaw Field Station during periods when no snow was falling.

Gerdel and Diamond (17), from their measurements on the Greenland Ice Cap, showed that a mean daily cloud cover of 0.5 reduced the incident total solar radiation by only 6%, and, even during completely overcast conditions, the snow surface received 65% as much solar radiation as on a clear day. Thams, as reported by Hoeck (18), made a similar study and found that daily solar radiation decreased at an increasing rate with increasing cloudiness, and with completely overcast skies averaged 24% of the clear sky radiation. These results are not strictly comparable with the Keweenaw Field Station results since the percentages are based on clear sky data. A check of the latter data shows, however, that radiation measured with overcast clouds at less than 5000 feet averaged about 70% of the clear sky radiation.

b) Reflected Solar

Snow Albedo - The albedo is defined as the ratio of the short-wave radiation energy reflected by the snow surface to that incident upon it. If the albedo is equal to zero, all incident radiation is absorbed, and if it is equal to one (or 100%), all incident radiation is reflected. Previous investigations (19) and (5) have shown that the variations of the snow albedo are dependent upon the character of the snow surface. Newly-fallen snow may reflect 80% or more of the incident solar radiation, while a ripe, granular snow may reflect as little as 40%. One of the greatest difficulties in establishing the relationship between albedo and the character of the snow surface is that the albedo is determined by a well-defined number whereas the character of the surface is impossible to define quantitatively. As a result, it is necessary to describe the most obvious changes of the snow surface to establish their relationship with changes that are liable to occur in the albedo.

In general, the albedo of snow decreases with snow compaction and with increasing size of snow crystals on the surface. Its daily variations thus depend mainly on (1) air temperature, (2) radiation intensity, and (3) the age of the snow. Positive air temperatures and intense solar radiation hasten the compaction process and thus decrease the albedo by increasing the concentration of liquid water in the top layers of the snow. Following is a summary of factors which produce an increase or a decrease in the albedo (See Reference 5).

Increase of the albedo by:	Decrease of the albedo by:
(1) New snow	(1) Snow cover becoming denser
(2) New formation of crystals by freezing of the surface	(2) Crystalline transformation, if accompanied by a coarsening of the crystals
(3) Sublimation of the surface	(3) Thawing of the surface

The frequent, almost daily, snowfalls at persistent temperatures below 0°C at the Keweenaw Field Station maintained daily albedos at about 90% in January and 85-90% late in February. Also conducive to the high albedos were the strong winds that commonly accompanied snowfalls. Such conditions caused the drifting snow to become ground or polished into rounded small particles, a few hundredths to a few tenths of a millimeter in diameter. The highest albedos at the Keweenaw Field Station were measured in overcast conditions following a snowfall, during which air temperatures were well below 0°C and the snow surface was wind-packed and fine grained. Overcast albedos exceeded clear-sky albedos by an average of 2-5%.

2. LONG WAVE RADIATION

Long wave (terrestrial and atmospheric) radiation is generally included in the electromagnetic spectrum between 3 microns and 80 microns. Radiation from the snow fills the spectrum in a continuous manner, whereas atmospheric radiation has a band-like character as long as the sky is not covered by clouds. Because a clear atmosphere does not absorb significantly in the range between 9 microns and 12 microns, the energy radiated by a snow cover within this range passes through the atmosphere.

a) Snow Radiation

Snow is very nearly a perfect black body with respect to long wave radiation, absorbing nearly all such radiation incident upon it and emitting the maximum possible radiation at its surface temperature in accordance with Stefan's Law. The surface temperature depends on the heat exchange of the snow surface with the atmosphere on the one hand (through radiation, conduction and convection), and with the interior of the snow on the other. The coefficient of emissivity of snow is given at nearly unity for long wave radiation by Falckenberg as reported by Eckel and Thams (5). If the radiation constant of $\sigma = 8.26 \times 10^{-11}$ ly/min/deg^4 is used, the maximum intensity of radiation that may be emitted by it is 0.459 ly/min (660 ly/day), since the temperature of snow is limited to a maximum of 0°C.

b) Atmospheric Radiation

Variation in the long wave radiation of the atmosphere depends largely on variations in cloudiness. For a cloudless atmosphere the variations are dependent on the temperature and water vapor content variations at all layers above the snow surface. The greater the water vapor content and the higher the atmospheric temperature, the higher will be the atmospheric radiation flux toward the snow.

Clear Nights - At night, the atmospheric radiation component is measured directly by the total hemispherical radiometer. A first step to relate measured atmospheric radiation to meteorological conditions at the Keweenaw Field Station was carried out for clear nights. Approximately 180 hourly totals of atmospheric radiation were found to be closely related to the hourly air temperatures reported by the adjacent weather station. A scatter diagram illustrating this relationship is shown in Figure 3. Values ranged from an atmospheric component of about 11 ly/hr with a shelter temperature of -26°C to about 21 ly/hr with a shelter temperature of -2°C. Also shown in the figure are values of total energy emitted by a black body according to the Stefan-Boltzman Law. The slopes of the two curves are quite similar, with an average 7 ly/hr difference in absolute values.

Effects of Cloudiness - In the daytime the total hemispherical radiometer measures both atmospheric and solar radiation. In the following analysis, hourly totals of total radiation were grouped in the same cloudiness categories as used in the solar radiation analysis. Averages of hourly totals within each cloudiness category were computed. The resulting diurnal patterns representing the last two weeks in January and the entire month of February are shown in Figures 4 and 5. The data represent periods during which no snow was falling. If atmospheric radiation fluxes are computed by subtracting hourly values of incident solar from corresponding values of total radiation, its diurnal pattern as a function of cloudiness is given.

From differences between curves it can be seen that the atmospheric radiation during clear sky conditions is about 9 ly/hr less than corresponding values with low overcast cloudiness. Such a clouding-over destroys the balance between the three energy fluxes at the snow surface that exists with clear skies. A thick cloud cover radiates practically as a black body with a temperature nearly equal to that at the cloud base. Because the clouds are generally situated well above the main portion of the surface inversion, their temperature is initially higher than that of the snow surface. In addition, the window in the emission spectrum of atmospheric radiation closes as cloudiness increases to low overcast. The result is a higher radiation flux emitted downward by the cloud than the total radiation flux emitted upward by the snow surface. Thus, the net long wave radiation exchange of the snow surface in connection with a clouding-over changes sign; an energy loss becomes an energy gain. Because of this reversal, the temperatures of the air and the surface increase, the inversion disappears, and the snow surface, cloud base and the atmosphere between them attain nearly the same temperature. The net long wave radiation exchange is then nearly zero, for both cloud base and snow surface are radiating equally in the long wave spectrum, and the radiation is entrapped in the atmospheric layer separating cloud and snow. As a consequence of such a condition, strong surface temperature inversions that might have persisted prior to an overcast are destroyed and a slight lapse condition commonly replaces them. With low overcast cloudiness, the net longwave exchange averaged about -17 ly/day in January to -8 ly/day in February. With clear skies, the net longwave exchange averaged about -128 ly/day in January to -120 ly/day in February.

The temperature rise of the snow surface is aided not only by turbulent heat transfer before an inversion disappears, but also initially by the heat conduction in the snow, whose sign is gradually reversed, i.e., heat is conducted into the snow when the surface temperature increases sufficiently. The temperature of the surface layers of both air and snow increase until all three energy fluxes are negligibly small. A time is reached when, for all practical purposes, the cloud base and snow surface are in radiational equilibrium. Similar conditions were reported for the Antarctic by Liljequist (20).

During days with snow falling, and cloud conditions similar to those of the "no snow" analysis, average hourly values of total hemispherical radiation are about 5 ly/hr greater during midday for both January and February as shown in Figure 6. Such an increase is indicative of the effect of greater atmospheric water content.

3. NET RADIATION EXCHANGE

The net radiation exchange at the snow-air interface is defined by the difference between the total all-wave radiation flux downward to the snow surface and the total all-wave flux upward from the snow surface. The former consists of incoming solar and atmospheric radiation; the latter consists of reflected solar radiation and radiation emitted by the snow surface. The net radiation exchange, considered to be positive when the incoming radiation is greater than the outgoing (usually positive in daytime and negative at night) must balance the sum of (1) the energy involved in the change of state of snow at its surface, (2) the conduction of heat in the snow, and (3) the turbulent transfer of sensible heat between the atmosphere and the snow surface.

If all radiation fluxes directed toward the snow are considered positive and those directed away are considered negative, the radiation balance may be written:

$$N = (1-A)\ I_o - (E-G)$$

where: N = net all-wave radiational gain (+) or loss (-) by the snow,
A = albedo of the snow surface,
I_o = incoming short-wave radiation,
E = outgoing long wave snow radiation,
G = incoming long wave atmospheric radiation.

The term (E-G) comprises the net long-wave exchange.

a) Effects of Cloudiness

Net radiation measurements for the two snow seasons were analyzed similarly to other components of the radiation balance. The results, shown in Figures 4 and 5, present average diurnal patterns of net radiation as a function of cloudiness for the last two weeks of January and the entire month of February. Again, data represent periods during which no snow was falling.

Net radiation is shown to decrease with a decrease in cloud amount during midday periods despite an increase in solar radiation. This somewhat paradoxical result can be discussed in terms of the equation for net radiation. As the cloud amount decreases, the atmospheric radiation component (G) also decreases. The difference between conditions of overcast clouds below 5000 feet and clear skies is about 9 ly/hr. The maximum hourly value of solar radiation (I_o), however, increased approximately 35 ly/hr during the same change in cloudiness, but about 90% of this amount was reflected by the snow. On the other hand, snow absorbed nearly all of the incoming long wave component and radiated upward according to its surface temperature. Thus, as skies cleared, the net long wave exchange (E-G) decreased sharply because the atmospheric component decreased and because the window in the emission spectrum of atmospheric radiation opened wide, enabling an increased amount of radiation to escape unintercepted by clouds. The decrease in net outgoing long wave radiation and the high albedo of snow for short wave radiation maintained average net radiation values slightly negative with clear skies during midday in January and slightly positive in

February. During nighttime conditions, net radiation decreased with a decrease of cloud amount more noticeably because of the absence of solar radiation.

The cloudiness categories between low overcast and clear skies show an uncertainty with respect to net radiation during the daytime. As cloud heights rose and cloud amounts decreased, the tendency was for net radiation to decrease slightly. Generally, results indicate that any midday cloudiness resulted in a positive net radiation. Enough solar radiation permeated the clouds, their warmer daytime moisture provided enough atmospheric radiation, and yet they intercepted enough snow radiation to achieve a slightly positive (incoming) net radiation.

The highest positive values of net radiation occurred during the daytime with low overcast or broken cloudiness and snow, shown in Figure 6. As previously discussed, the net long wave radiation becomes almost nil under low overcast conditions. During the daytime the diffuse short-wave sky radiation acts as a heat source for the snow surface, even if the sky is overcast. It is conceivable that during a snowfall the snowflakes possess a higher temperature (heat released by condensation) than the lower atmospheric layers. In addition, the increased atmospheric moisture content is conducive to an increase in the long wave atmospheric radiation component.

Many factors are left open to question. Cloud observations were subjective in most cases, and thicknesses were not considered in the analysis. The cloud climatology at the Keweenaw Field Station necessitated that cloud observations be grouped into categories which included a large range in cloudiness conditions in order to obtain enough representative samples in each category. And, finally, for a similar reason, longer time periods than desirable (one month in the case of February) were necessary for the averaging interval.

Table 1

MEASURED SOLAR RADIATION vs. CLOUDINESS

Average Measured Daily Insolation in per cent of that received outside the earth's atmosphere	Average Cloudiness	
	Half Day Combinations	Whole Day
80 - 90		Clear or hi sctd
70 - 80	Less than 3000 ft ovcst or brkn and less than 3000 ft sctd or clear	Greater than 5000 ft broken
60 - 70	Less than 3000 ft ovcst and less than 3000 ft brkn	Greater than 5000 ft ovcst
50 - 60	Less than 1000 ft ovcst and light snow and greater than 5000 ft brkn	Less than 3000 ft brkn vrbl ovcst and light snow
40 - 50	Less than 1000 ft ovcst and light snow and less than 2000 ft brkn	Less than 3000 ft ovcst and light snow
30 - 40		1000 - 2000 ft ovcst and snow
Less than 30		Less than 1000 ft ovcst and snow

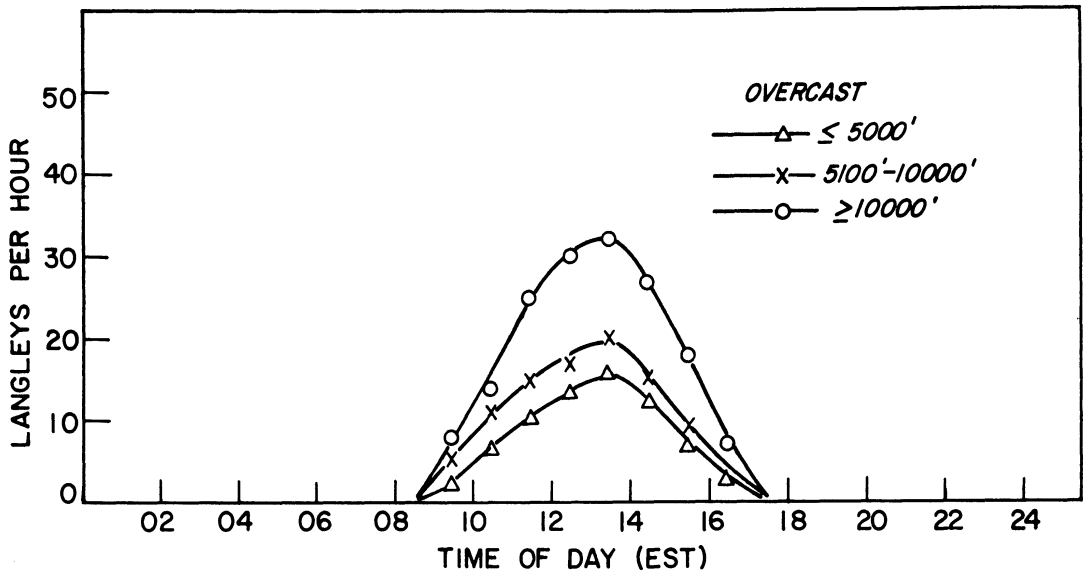

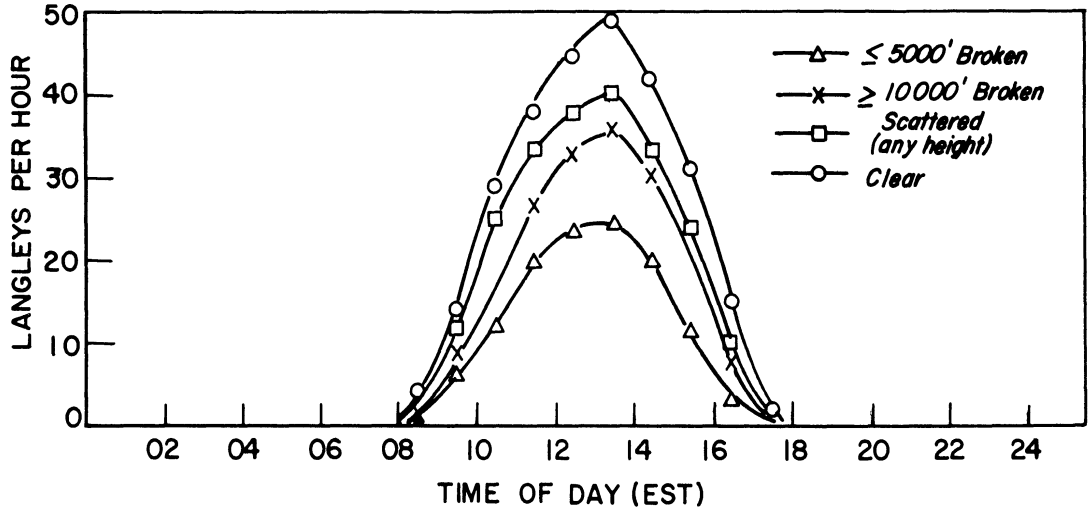

Fig. 2. Average Diurnal Patterns of Total Solar Radiation for January 15-31 for Different Cloud Conditions.

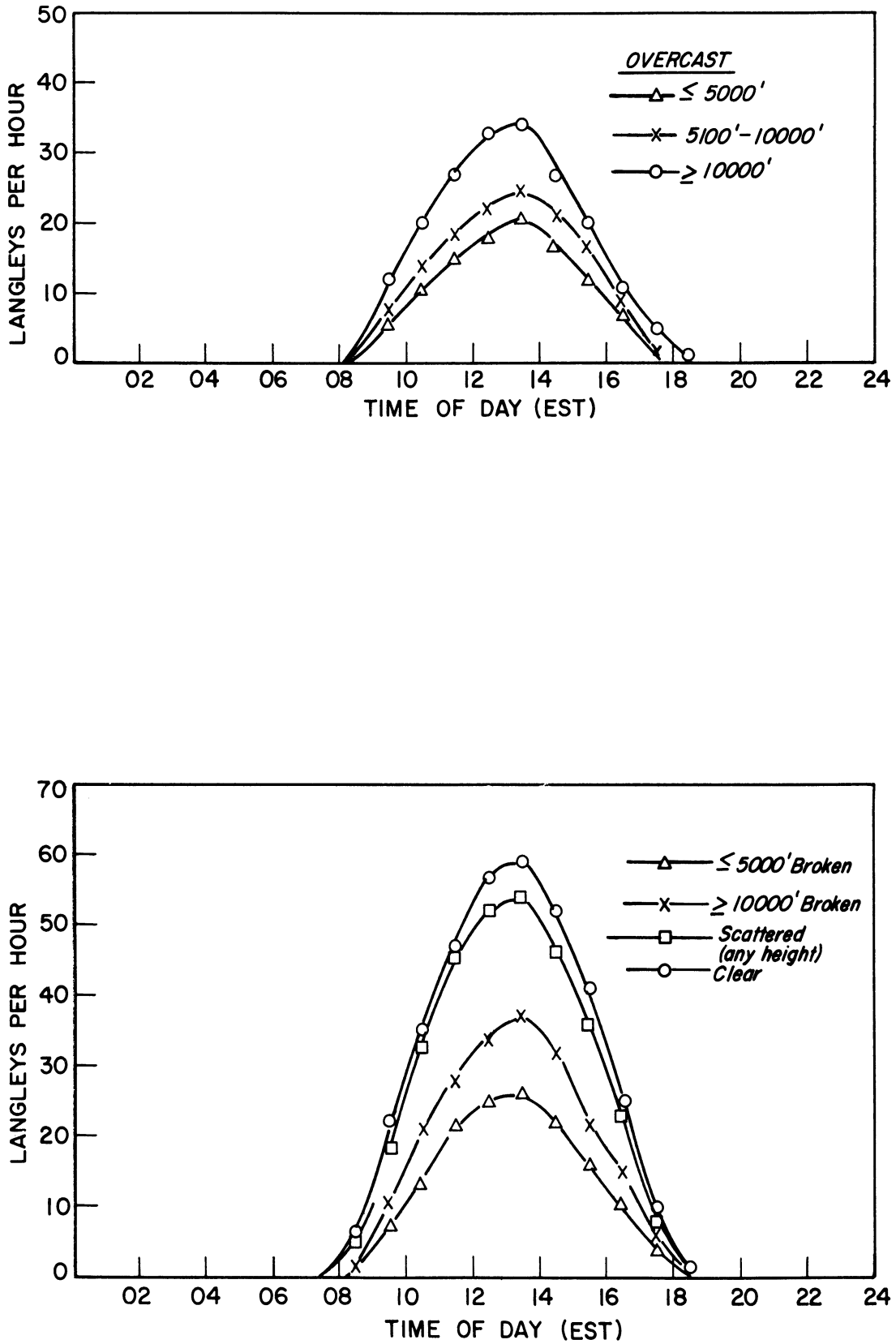

Fig. 2a. Average Diurnal Patterns of Total Solar Radiation for February for Different Cloud Conditions.

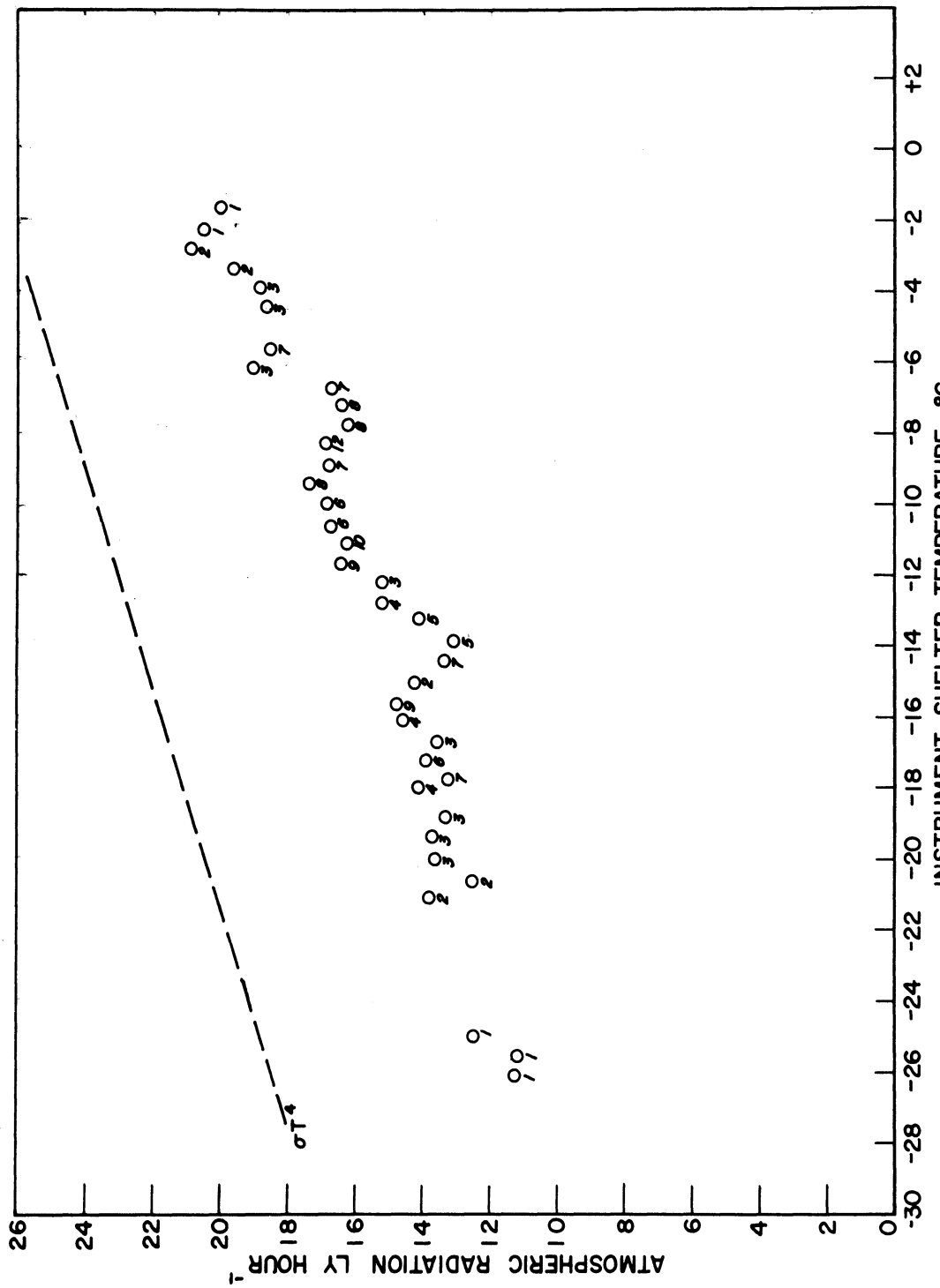

Fig. 3. Atmospheric Radiation versus Instrument Shelter Temperature with Clear Nocturnal Conditions. (The number of cases averaged for each point is indicated below it.)

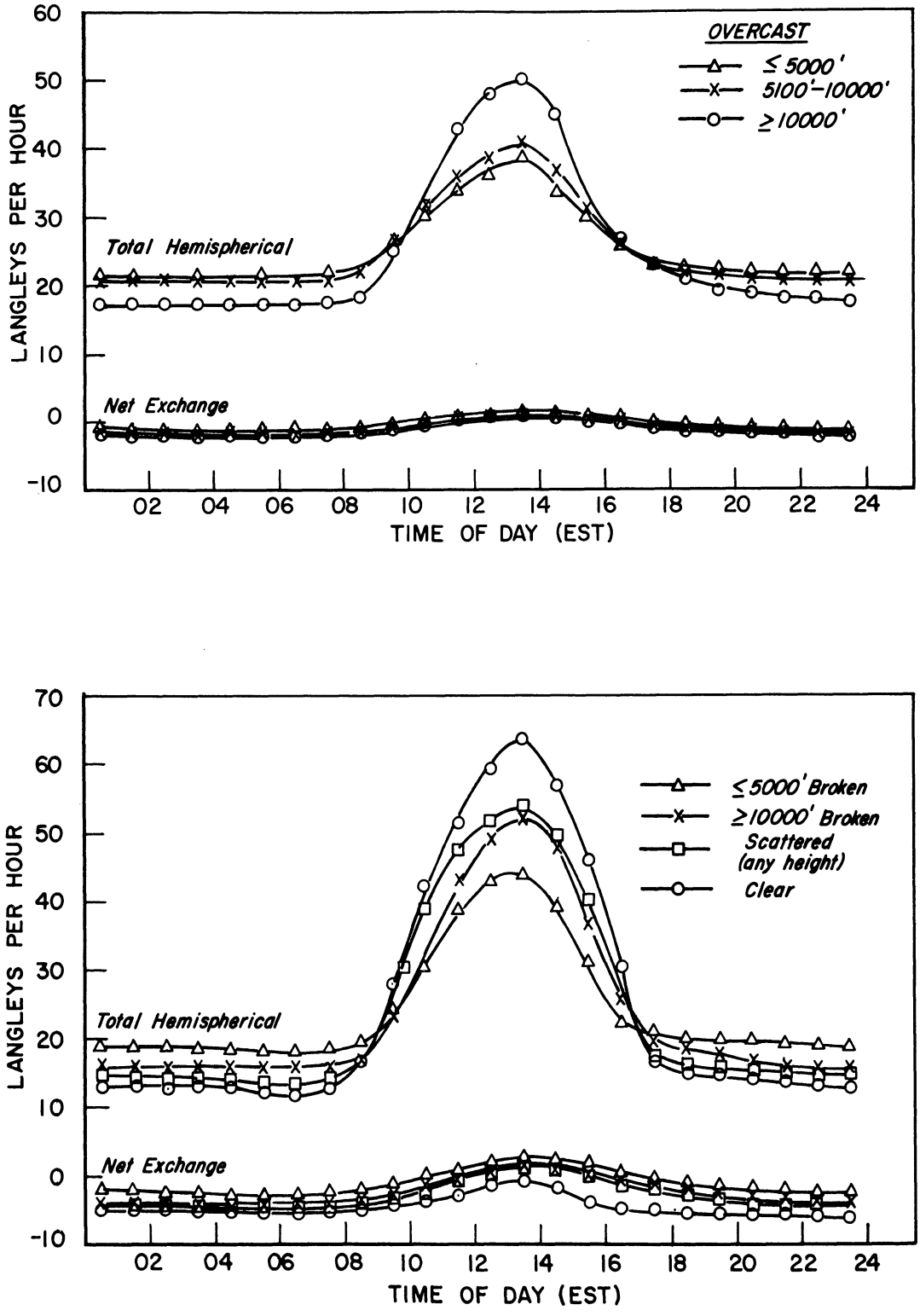

Fig. 4. Average Diurnal Patterns of Total Hemispherical and Net Radiation Fluxes for January 15-31 for Different Cloud Conditions.

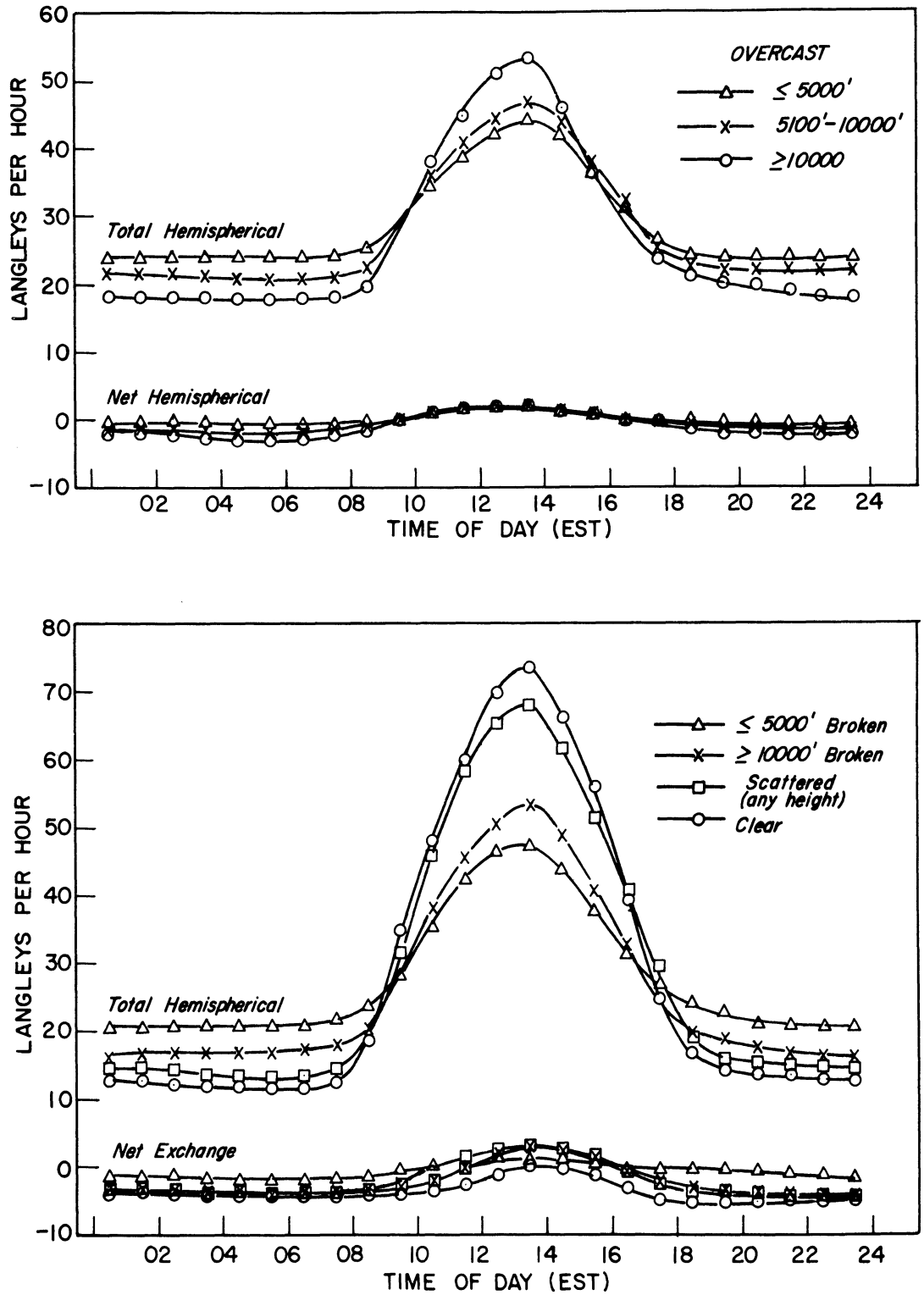

Fig. 5. Average Diurnal Patterns of Total Hemispherical and Net Radiation Fluxes for February for Different Cloud Conditions.

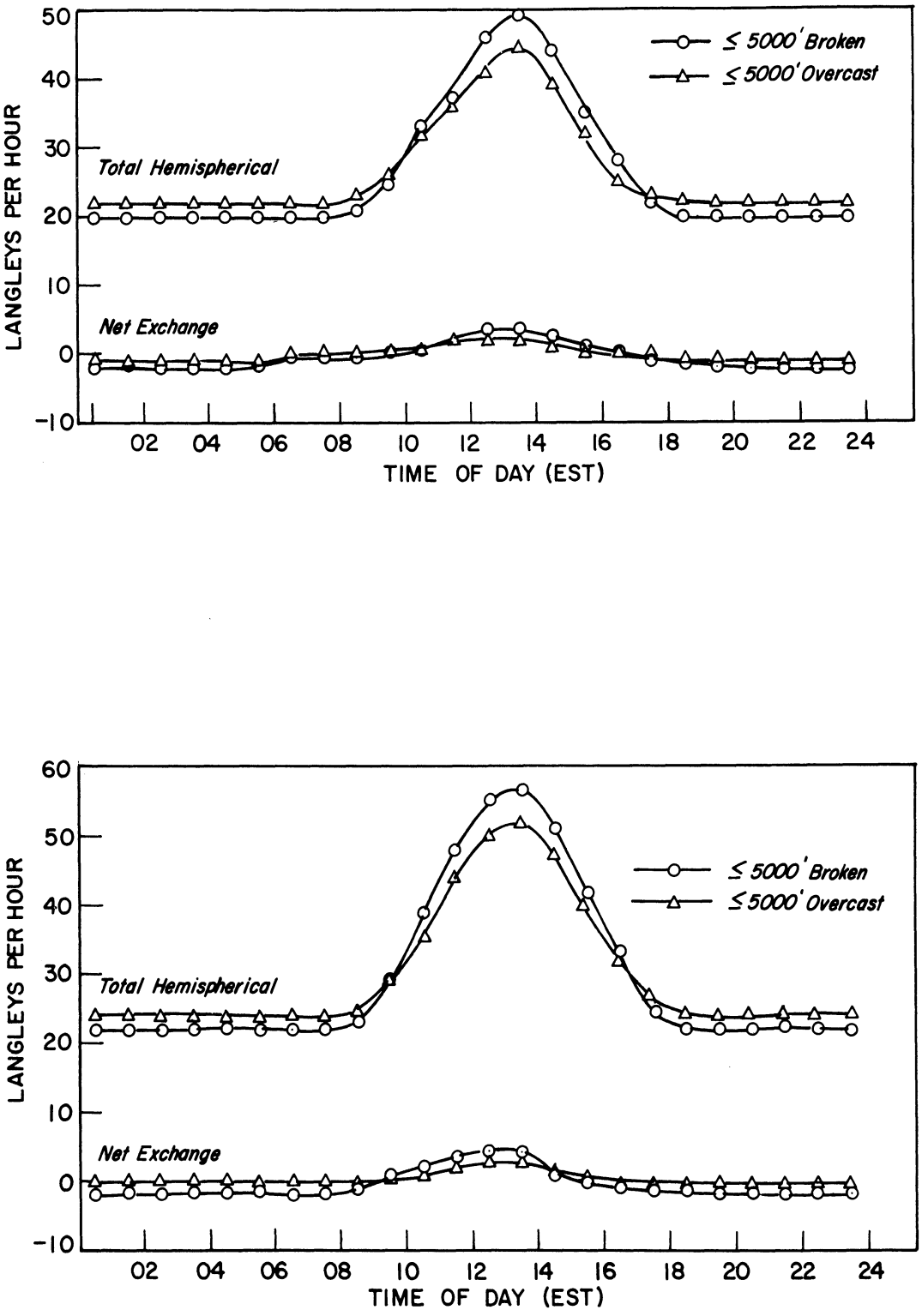

Fig. 6. Average Diurnal Patterns of Total Hemispherical and Net Radiation Fluxes for January 15-31 (upper) and February (lower) for Different Cloud Conditions with Snow Falling.

D. CONVECTIVE HEAT TRANSFER

Vertical motions in turbulence in the surface layer of the atmosphere are responsible for the transfer of properties between the atmosphere and the snow surface. In the absence of density stratification in the surface layer, the vertical motions are controlled by (1) the variation with height of the average wind speed (i.e., wind shear) and (2) snow surface roughness. Influences of density stratification are important, however, since a snow surface may seldom be at the same temperature as the air moving over it, that is to say that convective heat transfer is seldom zero, for significant periods of time. When the mean temperature (or more correctly the potential temperature) decreases with height in the surface air layer buoyancy effects are very important in contributing to and determining the characteristics of the vertical motion. In the opposite condition, when the potential temperature increases with height, the effects of buoyancy tend to inhibit vertical motions. The latter case is the more important one for most snow surfaces.

For a given roughness the relative significance of wind shear and density, or temperature, stratification on vertical motions can often be estimated from the mean wind speed at a reference height and the amount and height of cloudiness The influence of cloudiness, day or night, follows directly from the fact that the radiative transfer processes are largely responsible for maintaining the snow surface at a temperature different from the air flowing over it. For low net radiative transfer and windy conditions buoyancy effects are absent or nearly so. At the other extreme, with a large amount of net radiative heat transfer and with very light or no wind, wind shear is absent and vertical motions are entirely controlled by buoyancy effects. The first condition is comparable to the "forced convection" regime in engineering heat transfer problems and the second condition with the snow temperature greater than that of the air is comparable to the "free convection" situation. The second condition with snow temperature less than the air temperature appears not to have been widely treated in engineering problems.

Computation or estimation of the vertical fluxes of heat, water vapor and momentum in the surface layer of the atmosphere have generally avoided the use of direct information on vertical motions since these are extremely difficult to measure and have resisted specification for general application on a theoretical basis. The alternate approach is through the exchange coefficient hypothesis which seeks to relate the mean flux of momentum, heat or water vapor to the mean vertical gradient of the appropriate quantity (wind speed, temperature or water vapor pressure) by means of a transfer coefficient. The latter approach has proved successful for the specific situation of steady wind shear without buoyancy effects through the well-known Prandtl-Karman logarithmic relationship between wind speed and height. Thus it is possible to determine a momentum transfer coefficient in the absence of potential temperature stratification (i.e., in adiabatic conditions) merely from the measurement of mean wind speed at two heights above the surface. The analysis yields simultaneously, information on the roughness characteristics of the surface. The application of the adiabatic momentum transfer coefficient to heat transfer, of course has no meaning but its application to water vapor transfer through knowledge of the vapor pressure gradient is a question that is still under debate.

For the free convection condition, in the absence of a mean wind shear, Priestley (21) has proposed a relationship between temperature gradient and heat flux which, presumably, permits the direct calculation of the latter with the assumption of the value of only one arbitrary constant. At the

other extreme condition, i.e., no wind shear and temperature increasing with height, (i.e., inversion condition) turbulence would be absent and the transfer of heat, momentum and water vapor must proceed at rates determined by their respective still-air diffusion coefficients. Most observations indicate that both extreme conditions are essentially transitory and that only the latter is likely to have much significance for heat transfer to and from a snow cover.

The current status of the exchange coefficient hypothesis for conditions intermediate between the adiabatic and the extreme lapse and inversion conditions rests largely with the validity of assumptions of similarity between heat and momentum transfer, for various degrees of buoyancy influence. The Monin-Obukhov (6) treatment of the problem assumes (1) equivalence of the transfer coefficients for heat and momentum and (2) that for near-adiabatic conditions the relationship between wind speed and height can be expressed with the faimilar Prandtl-Karman logarithmic law with an additional term. The latter involves a constant coefficient and a characteristic length which, in turn, involves heat flux. Since the potential temperature may be similarly expressed, the characteristic length may be eliminated from the simultaneous equations. Thus, one is able to compute a transfer coefficient from knowledge of only wind and temperature gradients.

Aside from the assumption of equivalence of transfer coefficients for heat and momentum, successful application of the Monin-Obukhov relationships depends on (1) the numerical value of the coefficient and (2) whether or not they adequately describe conditions significantly different from adiabatic. Although there appears to be increasing evidence that the Monin-Obukhov model is satisfactory for lapse conditions not too far from adiabatic, Priestley (21) and Ellison (22) have discussed considerations which suggest that relationships of this type are unlikely to be appropriate for inversion conditions.

The special case of inversion conditions over snow surfaces has received considerable attention. The most recent work of significance is that of Liljequist (9) (10) who derived relationships for computing heat transfer for both moderate and large inversion conditions on the basis of an extensive series of wind and temperature profiles measured in the Antarctic. In deriving the relationships two basic assumptions were made: (1) that the transfer coefficients for heat and momentum are identical and (2) that the wind profile can be represented by the Prandtl-Karman logarithmic law with the addition of a linear term. The linear term was determined to be an exponential function of the degree of stability, i.e., the magnitude of the inversion. In many respects the Liljequist model is not greatly different from that of Monin and Obukhov. The derivation of the latter is more acceptable on a physical basis, but since the Liljequist model was formulated specifically to describe inversion conditions over snow it is especially attractive for the present study.

The two models have not been adequately tested by other workers and, until they are, evaluation of their utility cannot be made. The fact that testing such hypotheses requires very careful field observations seriously impedes prompt acceptance or rejection. The difficulty lies in two areas: (1) accurate measurement of wind and temperature profiles and (2) independent measurement or determination of the heat flux. The significance of the measurement problems for developing useful heat transfer relationships is probably greater than is generally recognized.

A consideration of the basic problem of turbulent transfer leads necessarily to the conclusion that at present there are no completely satisfactory

relationships for determination of turbulent heat transfer to a snow surface. Derivations such as those just reviewed may serve a practical purpose, however, and may, at least, reveal the relative significance of the convective heat transfer term for snow metamorphic processes.

1. LILJEQUIST METHOD

The Liljequist model (9) (10) for turbulent heat transfer in stable conditions over snow assumes identical exchange coefficients for both heat and momentum and the validity of the equation

$$Q = c_p \rho K \frac{\partial \theta}{\partial z} \qquad (1)$$

where: Q = heat flux (cal cm^{-2} sec^{-1})
c_p = specific heat at constant pressure (gr cal gr^{-1} deg^{-1})
ρ = density of air (gr cm^{-3})
K = eddy conductivity = eddy viscosity (cm^2 sec^{-1})
θ = potential temperature (°K)

Moreover, in applying this equation, Liljequist has chosen practically linear temperature profiles up to 10m, but points out that turbulent heat transfer is not significantly different for other types of temperature profiles. To compute eddy viscosity, K, from wind data, Liljequist introduces a parameter, k', which is a measure of the linearity of the wind profile. His expression for the wind-height variation over snow may be represented by the following:

$$u = \frac{u_*}{k} \ln \frac{z + z_o}{z_o} + k'^2 z$$

which in terms of the 10 meter wind speed becomes

$$u = u_{10} \left[\left(\frac{1 - k'}{\ln Z/z_o} \right) \left(\ln \frac{z + z_o}{z_o} \right) + \frac{k'}{Z} z \right] .$$

The notation is as follows:

u = wind speed at level z
u_{10} = wind speed at 10 meters
u_* = friction velocity
Z = reference level of 10 meters
z_o = roughness parameter
k' = linearity parameter
k = the Karman constant = 0.40
ln = natural logarithm

With k' = 0 the wind profile is logarithmic. With steadily increasing stability, turbulence is suppressed to a greater degree and the wind profile approaches linearity, i.e., k' approaches one. In other words, if stability increases from zero (neutral stability), k' increases from zero towards one, and the wind profile changes from logarithmic toward linear. The functional relation between k' and stability was obtained by analyzing about 100 wind

profiles under various stability conditions.

Two interpolation formulas are given for k': an exponential and a linear expression. When applied to heat transfer computations, the exponential expression gives a more rapid increase in heat transfer with increasing stability. Liljequist points out, however, that within the stability regions most commonly observed over snow in high latitudes, nearly the same heat transfer computations are obtained from both expressions. The results obtained from the exponential expression were employed in this analysis.

His computations of eddy viscosity show a rapid decrease as stability increases. With neutral stability, K increases linearly with height. With stratified air, K also increases with height, but approaches a limiting value asymptotically. A table is given showing eddy viscosity with u_{10} = 1m/sec for different stability conditions and heights above snow.

Stability (S) is defined by $\frac{g}{\theta}\frac{\partial \theta}{\partial Z}$, or $\frac{\partial \theta}{\partial Z} = \left(\frac{263}{980.8}\right)(S)$ represents average conditions at the Keweenaw Field Station. If pressure is assumed constant, $\frac{\rho}{\rho_o} = \frac{\theta_o}{\theta}$, where ρ_o is the density at θ_o = 273°K and at the average wintertime atmospheric pressure at the Keweenaw Field Station, which is about 990mb, then

$$\rho_o = \frac{990}{1013.2}\ (1.293\text{x}10^{-3}) = 1.262\text{x}10^{-3}\ \text{gcm}^{-3}$$

Substituting these expressions in eq. (1) yields

$$Q = c_p\ \rho_o\ \frac{\theta_o}{g}\ (60)(S)(K)\ \text{ly/min}$$

where: $c_p = 0.24$ (gr cal gr^{-1})
$\rho_o = 1.262\text{x}10^{-3}$ (gr cm^{-3})
$\theta_o = 273$ (°K)
$g = 980.8$ (cm sec^{-2})

and finally

$$Q = (.24)(60)(1.262\text{x}10^{-3})\ \frac{273}{980.8}\ (S)(K)$$

From the table given by Liljequist, values for the products SK valid for a wind speed of 1m/sec at 10 meters and a height of 5 meters were obtained. Choosing values of K at a height of 5 meters compensates for curvature in temperature profiles that might exist at the lowest levels during low stability conditions, since the temperature gradient was determined from linear profiles. Thus, $Q = Q_1\ u_{10}$, and with u_{10} = 1m/sec, Table 2 gives the turbulent transfer of heat as a function of stability.

Table 2

TURBULENT TRANSFER OF HEAT VERSUS STABILITY

$S \times 10^{-2}$ sec^{-2}	K $cm^2 sec^{-1}$ z=5m u_{10}=1m/sec	$\frac{\partial \theta}{\partial Z}$ °C/m	Q_1 ly/min for u_{10}=1m/sec
0	7025	0	0
.1	586	.027	.0029
.25	365	.067	.0046
.5	211	.134	.0054
1.0	114	.268	.0059
6.0	19.4	1.61	.0059

Average multiplying factors (Q_1) within designated stability intervals obtained from Table 2 are shown in Table 3.

Table 3

MULTIPLYING FACTORS (Q_1) OF 10 METER WIND SPEEDS

Temperature Difference ($T_{10m}-T_{1m}$ °C)	Code	Average Q_1 Ly/min	Ly/hr
Lapse	L		
Adiabatic	0		
0.1-1.0	1	0.0044	0.264
1.1-2.0	2	0.0055	0.330
2.1-3.0	3	0.0058	0.348
3.1-4.0	4	0.0059	0.354
4.1-5.0	5	0.0059	0.354
5.1-6.0	6	0.0059	0.354
6.1-7.0	7	0.0059	0.354
7.1-8.0	8	0.0059	0.354
8.1-9.0	9	0.0059	0.354
9.1-10.0	10	0.0059	0.354
Greater than 10	11	$\cong$ 0.0059	$\cong$ 0.354

Thus, for stability values greater than $10^{-2} sec^{-2}$ ($\partial\theta/\partial Z$ greater than about 0.27°C/m) and for a constant wind speed at 10 meters, the turbulent flux of heat remains nearly independent of the temperature gradient and $Q = Q_1 u_{10}$ $= .0059\ u_{10}$ ly/min. The flux of heat downward to the surface becomes directly proportional only to the wind speed at a reference level (10 meters) for well-developed inversions, i.e., greater than about 2.7°C per 10 meters.

Wehn an inversion gradually replaces neutral stability, a simultaneous rapid increase in heat transfer occurs with increasing inversion magnitude until the stability reaches $10^{-2} sec^{-2}$. The significance of this lower stability region becomes important in that small temperature inversions that may accompany fresh or strong winds cause a moderate heat transfer in spite

of their relatively small magnitude.

The dependence of the temperature profile over snow upon wind speed and cloudiness at KFS was studied separately for daytime and nocturnal (nighttime) conditions. To obtain temperature differences, interpolation was necessary in many profiles, which suggested the use of class intervals of the temperature differences listed in Table 3. The hourly mean temperature difference between 10 meters and 1 meter for 21 days in 1956 was related to wind speed and cloudiness measured by the FAA weather station. Days during which no snow fell were selected, since snow commonly collected in the anemometer cups during snowfalls. Results are summarized in Table 4. Each temperature difference represents an average for that particular category.

The table is conspicuous by the near disappearance of the inversion during the day, which was commonly replaced by a slight temperature lapse. Such an occurrence causes the turbulent heat transfer to decline to zero ($\Delta T/\Delta Z=0$) or even to reverse its sign ($\Delta T/\Delta Z < 0$) i.e., heat transfer away from the snow surface occurs. A temperature lapse averaging 0.1° to 0.5°C in 10 meters occurred most frequently during low overcast cloudiness and moderate winds; a condition substantiated by the simultaneous occurrence of the largest positive values of net radiation. Furthermore, with wind speeds above about 12 knots at KFS temperature profiles remained nearly adiabatic.

The same days analyzed for temperature profile dependence upon weather conditions were subjected to hourly heat transfer computations employing the Liljequist method. Each hourly computation was then categorized according to the prevailing cloud condition and wind speed at 10 meters. The computations represent turbulent heat transfer occurring during actual weather conditions, that is, conditions during which inversions were formed and broken up as a function of radiation and wind speed. Therefore, nothing more refined than quantitative estimates are presented in Table 5.

Table 6 lists the turbulent heat transfer computational data using the Liljequist method.

2. MONIN-OBUKHOV METHOD

Basic to the transfer coefficient hypothesis for turbulent transfer in the presence of a steady mean wind shear is the assumption of the existence of a layer of air near the surface in which the fluxes of heat, water vapor and momentum are essentially invariant with height. The maximum depth of such a layer varies with conditions. With a geostrophic wind of about 10 meters per sec and a tolerance of 20% permitted, Monin and Obukhov (6) estimate that the height of the constant-flux layer is 50 meters. Other workers might take exception to this value, but most would agree that, with a wind speed of a few meters per second at any height within the layer, the layer would be at least 8-10 meters deep.

Monin and Obukhov describe the wind and temperature profiles in the constant flux layer as follows:

$$\partial u/\partial z = \frac{u_*}{kz}\,\phi_1\,(z/L) \qquad (1)$$

and

$$\partial \theta/\partial z = \frac{T_*}{kz}\,\phi_2\,(z/L) \qquad (2)$$

in which ϕ_1 and ϕ_2 are undetermined functions, and

$$L = u_*^3/k(g/T)(Q/\rho c_p) \tag{3}$$

$$T_* = -Q/\rho c_p u_* \tag{4}$$

The remainder of the notation is the same as that used in discussing the Liljequist model. It should be noted that equation (1) is the same as the adiabatic wind profile with $\phi_1(z/L) = 1$.

It is assumed not only that the wind and temperature profiles are similar but, also (1) that the transfer coefficients for heat and momentum are equivalent and (2) that $\phi_1 = \phi_2 = \phi$. The only information on the nature of ϕ is that

$$\phi(z/L) \rightarrow 1$$

as $$Q \rightarrow 0$$

which is equivalent to

$$|L| \rightarrow \infty$$

thus $$\phi(0) = 1$$

The term $\phi(z/L)$ is developed in a power series,

$$\phi(z/L) = \phi(0) + \beta(z/L) + \ldots\ldots$$

and $$\simeq 1 + \beta(z/L)$$

for $z \ll |L|$. The coefficient β is taken to be a universal constant whose value was determined by Monin and Obukhov to be $-0.6 \pm 10\%$ from analysis of a large number of wind and temperature profiles.

Integration of Equations (1) and (2) gives

$$u_2 - u_1 = u_*/k\left[(\ln z_2/z_1) + \beta \frac{(z_2 - z_1)}{L}\right] \tag{5}$$

and

$$\theta_2 - \theta_1 = T_*/k\left[(\ln z_2/z_1) + \beta \frac{(z_2 - z_1)}{L}\right] \tag{6}$$

from which it is possible to eliminate L and T_* in order to compute u_* from appropriate wind and temperature data. Heat flux, then, is given by

$$Q = \rho c_p u_*^2 \frac{\theta_1 - \theta_2}{u_2 - u_1} \tag{7}$$

which follows from the defining relationship of u_* and K and the substitution of finite differences for differentials. It should be noted that Equations (5),

(6) and (7) depend very importantly on the restriction that $z \ll L$, which implies that measurements must be made very near the snow surface when the heat flux is large.

Equation (7) was used to compute several hourly values of sensible heat flux for each of six days in the 1955-56 snow season. The results are listed in Table 7. The specific periods were selected on the basis of (1) the appearance of the wind and temperature profiles and (2) the absence of precipitation. Negative values of heat flux indicate flux away from the snow surface. Heat flux values marked with asterisks were values for which friction velocities (u_*) were negative. A negative friction velocity was obtained when a temperature inversion was large in comparison to the wind shear, a condition that suggests important buoyancy effects. Stated another way, it indicates that the characteristic length, L, was too small to satisfy the requirement that z be significantly less than L. It could not be expected, therefore, that the Monin-Obukhov relationships would be appropriate for these conditions. The data are presented, nonetheless, to illustrate the apparent limitations of this model for various wind and temperature conditions.

The remainder of the computed heat flux values ranged from about -37 to +34 ly/hr with most of the values, however, between -2 and +3 ly/hr. There appears to be no direct relationship between these results and those obtained with the Liljequist model for the same periods. In the absence of direct information of the gains and losses of heat by the snow cover and of an independent estimate of the exchange of latent heat of change of phase for the same periods of time, it is impossible to decide which model gives the more correct results. Because of the severely restricted region of validity for the Monin and Obukhov model, as indicated by the many periods for which negative friction velocities were obtained, one is inclined to place more faith in the Liljequist model for the Keweenaw Field Station data.

Table 4

TEMPERATURE DIFFERENCES (T_{10m}-T_{1m}) vs. CLOUDINESS AND WIND SPEEDS
(Degrees Centigrade)

Night

FAA Weather Station Wind Speed (knots)	Overcast		Broken		Sctd or Clear
	Less Than 1000 ft to 5000 ft	Greater Than 5000 ft	1000 ft to 5000 ft	Greater Than 5000 ft	
0-3	1-2	1-2	2-4	3-5	6-8
4-7	0 or lapse	less than 1	1-2	2-3	3-4
8-11	"	0	less than 1	less than 1	1
greater than 11	"	0	0	0	0

Day

	Overcast at any Height	Broken at any Height	Sctd or Clear
0-3	Less than 1	Less than 1	1
4-7	0 or lapse	0 or lapse	Less than 1
8-11	"	"	0 or lapse
greater than 11	"	"	"

Table 5

TURBULENT HEAT TRANSFER vs. CLOUDINESS AND WIND SPEEDS
Langleys/Hour

Wind Speed at 10 Meters MPH	Overcast at any Height	Broken at any Height	Scattered	Clear
	Night			
0-3	0.1	0.2	0.2	0.3
4-7	0	0.5	0.6	0.7
8-11	0	0.8	1.0	1.2
greater than 11	0	0	0	0
	Day			
0-3	Less than 0.1	0.1	0.1	0.1
4-7	0	0	0.2	0.2
8-11	0	0	0	0
greater than 11	0	0	0	0

Table 6. TURBULENT HEAT TRANSFER (LILJEQUIST METHOD) AND TEMPERATURE DIFFERENCE DATA*

Time of Day	u_{10} m/sec	$T_{10m}-T_{1m}$ °C	Q ly/hr	u_{10} m/sec	$T_{10m}-T_{1m}$ °C	Q ly/hr	u_{10} m/sec	$T_{10m}-T_{1m}$ °C	Q ly/hr
	January 11, 1956			January 12, 1956			January 13, 1956		
01	6.03	L		2.03	4	.72	2.51	1	.66
02	5.72	L		2.20	6	.78	2.72	1	.72
03	5.63	L		2.46	6	.87	2.28	0	0
04	6.33	0	0	1.76	9	.62	2.99	L	
05	5.45	L		1.49	6	.53	2.81	L	
06	5.54	0	0	1.49	8	.53	2.72	1	.72
07	5.72	0	0	1.63	8	.58	2.07	1	.55
08	4.88	L		1.49	3	.52	2.03	1	.54
09	4.31	L		1.10	4	.39	1.01	1	.27
10	4.31	L		1.36	3	.47	1.63	0	0
11	4.62	0	0	1.84	2	.61	1.32	2	.44
12	4.62	0	0	1.28	1	.34	.88	1	.23
13	5.01	0	0	2.07	1	.55	1.32	L	
14	4.44	0	0	2.20	L		1.32	2	.44
15	3.56	0	0	2.99	L		2.16	1	.57
16	3.65	0	0	3.16	L		2.55	0	0
17	3.48	0	0	2.72	1	.72	2.95	2	.97
18	3.12	0	0	2.42	1	.64	1.76	3	.61
19	3.43	0	0	1.84	2	.61	1.98	3	.69
20	3.74	0	0	1.63	2	.54	2.11	3	.73
21	2.46	2	.81	.96	4	.34	1.84	3	.64
22	1.67	4	.59	1.45	1	.38	1.93	3	.67
23	1.93	3	.67	1.76	0	0	2.90	3	1.01
24	2.33	5	.82	1.76	1	.46	2.07	3	.72
	January 14, 1956			January 21, 1956			January 25, 1956		
01	3.48	2	1.15	2.55	0	0	.44	7	.16
02	4.40	1	1.16	2.90	0	0	.48	6	.17
03	2.46	2	.81	2.99	1	.79	.53	6	.19
04	2.95	1	.78	2.51	1	.66	Calm	6	0
05	2.77	2	.91	2.90	1	.77	Calm	4	0
06	2.03	2	.67	2.03	2	.67	.44	2	.15
07	2.68	3	.93	1.67	2	.55	Calm	2	0
08	2.90	1	.77	2.20	1	.58	.57	2	.19
09	2.37	1	.63	2.51	1	.66	.66	1	.17
10	3.92	0	0	1.84	2	.61	.92	2	.30
11	2.95	L		1.14	2	.38	1.32	1	.35
12	1.98	0	0	2.90	0	0	1.63	1	.43
13	2.90	L		2.37	L		1.59	L	
14	5.28	L		1.98	L		.79	L	
15	5.63	L		2.24	0	0	.79	0	0
16	5.10	L		2.55	1	.67	.88	1	.23
17	6.03	1	1.59	2.95	1	.78	1.67	1	.44
18	5.63	1	1.49	2.03	1	.54	1.84	2	.61
19	5.15	0	0	2.59	1	.69	1.40	6	.49
20	5.59	1	1.48	2.33	1	.62	1.89	5	.67
21	6.16	1	1.63	2.46	1	.65	2.03	7	.72
22	5.28	1	1.39	1.76	1	.46	2.11	10	.75
23	5.50	1	1.45	1.67	5	.59	1.67	9	.59
24	4.31	0	0	1.76	2	.58	1.76	11	.62

*See Table 3 for temperature difference code and multiplying factors.

Table 6. (Continued)

Time of Day	u_{10} m/sec	$T_{10m}-T_{1m}$ °C	Q ly/hr	u_{10} m/sec	$T_{10m}-T_{1m}$ °C	Q ly/hr	u_{10} m/sec	$T_{10m}-T_{1m}$ °C	Q ly/hr
	January 26, 1956			January 27, 1956			February 3, 1956		
01	1.01	9	.36	.88	3	.31	.79	11	.28
02	.44	11	.16	.70	5	.25	1.76	11	.62
03	Calm	11	0	.53	1	.14	1.76	11	.62
04	"	8	0	1.05	2	.35	2.63	8	.93
05	"	11	0	.53	3	.18	2.63	4	.93
06	"	11	0	.92	2	.30	2.63	2	.87
07	"	11	0	.53	7	.19	2.24	1	.59
08	"	11	0	.57	7	.20	2.68	2	.88
09	.44	10	.16	.53	10	.19	3.52	1	.93
10	.44	8	.16	.44	7	.16	5.63	1	1.49
11	1.01	2	.33	.48	3	.17	5.28	1	1.39
12	1.54	2	.51	.53	1	.14	3.34	1	.88
13	1.49	1	.39	.88	1	.23	2.51	1	.66
14	2.03	1	.54	1.67	1	.44	3.16	0	0
15	.88	1	.23	2.11	1	.56	2.07	1	.55
16	1.01	1	.27	3.87	1	1.02	3.34	0	0
17	1.32	4	.47	4.27	1	1.13	3.92	1	1.03
18	.88	6	.31	4.75	1	1.25	3.16	2	1.04
19	.44	9	.16	5.89	1	1.55	3.92	2	1.29
20	Calm	5	0	6.42	1	1.69	5.01	0	0
21	"	6	0	6.68	0	0	5.32	1	1.40
22	"	7	0	7.48	0	0	3.92	0	0
23	"	5	0	7.21	0	0	3.04	1	.80
24	44	4	.16	8.00	L		5.80	0	0
	February 4, 1956			February 5, 1956			February 6, 1956		
01	5.80	0	0	5.19	0	0	2.59	1	.68
02	4.66	0	0	5.24	0	0	4.00	1	1.06
03	4.57	0	0	3.74	0	0	4.13	1	1.09
04	4.53	0	0	2.86	0	0	4.31	1	1.14
05	4.18	0	0	2.95	0	0	4.83	0	0
06	4.18	0	0	2.03	1	.54	4.66	0	0
07	3.87	0	0	1.63	0	0	3.87	0	0
08	3.60	0	0	1.54	0	0	2.95	0	0
09	4.18	0		1.59	L		2.28	1	.60
10	4.79	0	0	1.76	1	.46	1.63	1	.43
11	4.57	L		2.11	0	0	2.99	1	.79
12	4.31	L		2.81	0	0	3.16	1	.83
13	5.80	L		2.37	0	0	2.68	1	.71
14	5.72	L		3.16	0	0	4.09	L	
15	6.16	L		3.48	0	0	4.40	0	0
16	6.95	0	0	3.16	0	0	4.00	0	0
17	5.45	L		3.25	0	0	3.21	L	
18	5.06	L		3.60	0	0	3.83	1	1.01
19	7.03	L		4.04	0	0	3.56	1	.94
20	5.94	L		5.10	1	1.35	3.12	1	.82
21	5.41	0	0	4.44	1	1.17	.44	6	.16
22	5.98	0	0	3.92	0	0	.66	10	.23
23	5.85	L		4.36	1	1.15	.70	11	.25
24.	5.89	1	1.55	3.25	1	.86	.66	9	.23

Table 6. (Continued)

Time of Day	u_{10} m/sec	$T_{10m}-T_{1m}$ °C	Q ly/hr	u_{10} m/sec	$T_{10m}-T_{1m}$ °C	Q ly/hr	u_{10} m/sec	$T_{10m}-T_{1m}$ °C	Q ly/hr
	February 7, 1956			February 8, 1956			February 9, 1956		
01	1.76	6	.46	5.72	0	0	2.99	2	.99
02	1.76	6	.46	5.63	0	0	3.39	1	.89
03	1.76	7	.46	4.92	L		3.78	1	.99
04	2.81	1	.74	4.75	L		3.87	2	1.28
05	3.30	0	0	3.04	2	1.00	2.51	3	.87
06	3.92	1	1.03	3.04	2	1.00	3.30	1	.87
07	4.13	L		2.81	0	0	4.75	0	0
08	3.56	L		3.34	0	0	4.83	0	0
09	2.99	L		3.52	L		6.56	1	1.73
10	4.44	0	0	3.34	L		6.51	0	0
11	4.48	L		4.13	L		6.77	1	1.79
12	3.08	L		4.75	L		5.68	L	
13	2.72	L		5.28	0	0	5.24	L	
14	2.77	1	.73	5.28	L		5.63	L	
15	3.16	1	.83	5.06	1	1.34	6.38	1	1.68
16	1.32	1	.35	5.28	0	0	6.42	1	1.69
17	2.63	L		5.63	0	0	6.16	1	1.63
18	3.25	0	0	5.36	0	0	6.07	0	0
19	5.10	1	1.35	4.31	1	1.14	6.16	1	1.63
20	6.60	0	0	2.81	1	.74	6.38	0	0
21	6.68	1	1.76	2.20	2	.73	6.51	1	1.72
22	6.56	1	1.73	2.33	5	.82	6.07	0	0
23	6.20	0	0	2.81	5	.99	5.54	1	1.46
24	6.33	L		2.81	2	.93	6.68	1	1.76
	February 23, 1956			February 28, 1956			March 1, 1956		
01	2.46	7	.87	1.76	4	.62	4.75	1	1.25
02	1.05	4	.37	3.65	2	1.20	5.72	1	1.51
03	2.20	7	.78	2.59	5	.92	5.36	1	1.42
04	1.89	9	.67	2.11	5	.75	6.73	1	1.78
05	1.76	11	.62	1.32	9	.47	7.21	0	0
06	1.63	11	.58	1.19	6	.42	6.56	1	1.73
07	.88	11	.31	1.05	6	.37	4.36	1	0
08	1.32	11	.47	1.49	6	.53	4.13	0	0
09	Calm	8	0	2.68	1	.71	2.77	1	.73
10	.48	2	.16	2.24	L		3.43	1	.91
11	.92	1	.24	2.59	L		2.99	1	.79
12	1.89	1	.49	3.08	L		5.01	0	0
13	1.76	1	.46	4.48	L		4.66	1	1.23
14	Calm	1	0	5.01	L		4.57	0	0
15	.48	1	.13	5.41	L		4.48	0	0
16	2.37	0	0	4.66	L		4.66	1	1.23
17	6.07	0	0	4.75	L		5.45	1	1.44
18	6.38	0	0	3.96	L		3.78	1	.99
19	5.76	0	0	3.12	1	.82	3.08	1	.81
20	4.57	0	0	3.25	1	.86	2.86	2	.94
21	4.92	L		3.87	1	1.02	2.46	2	.81
22	5.72	L		4.88	L		.92	8	.33
23	8.09	L		5.19	L		2.28	4	.81
24	7.26	L		5.41	L		3.65	1	.96

Table 6. (Continued)

Time of Day	u_{10} m/sec	$T_{10m}-T_{1m}$ °C	Q ly/hr	u_{10} m/sec	$T_{10m}-T_{1m}$ °C	Q ly/hr	u_{10} m/sec	$T_{10m}-T_{1m}$ °C	Q ly/hr
	March 2, 1956								
01	3.78	1	.99						
02	4.04	0	0						
03	2.86	0	0						
04	3.25	0	0						
05	3.60	0	0						
06	3.16	1	.83						
07	1.93	2	.64						
08	1.32	2	.44						
09	1.01	1	.27						
10	1.10	1	.29						
11	2.37	L							
12	3.43	L							
13	4.53	L							
14	4.31	L							
15	3.83	L							
16	2.68	L							
17	2.07	L							
18	1.19	1	.31						
19	1.49	1	.39						
20	Calm	4	0						
21	.75	6	.27						
22	.62	8	.22						
23	.70	7	.25						
24	.75	3	.26						

Table 7

TURBULENT HEAT TRANSFER DATA: MONIN AND OBUKHOV METHOD

Time of Day	Z_1 cm	Z_2 cm	u_1 cm/sec	u_2 cm/sec	θ_1 °C	θ_2 °C	Q ly/hr
			February 4, 1955				
15	259	559	413	462	-5.4	-5.7	-4.82
16			431	475	-6.0	-6.2	-3.03
17			290	339	-6.1	-6.6	-8.92
18			352	409	-5.8	-6.0	-3.51
19			483	515	-5.0	-4.6	+5.62
20			576	624	-4.8	-6.2	-36.72
21			638	677	-5.2	-6.3	-18.93
22			550	616	-4.4	-4.2	-3.53
23			792	872	-5.4	-6.7	-34.57
24			814	894	-5.0	-6.2	-31.13
			January 12, 1956				
02	150	333	140	154	-11.4	-9.4	+86.04*
03			184	193	-10.0	-8.4	+191.16*
04			96	132	-12.1	-6.5	+30.42*
05			96	119	-9.0	-6.5	+14.22*
06			79	96	-11.6	-8.1	+193.57*
07			136	159	-13.3	-10.1	+48.96*
			January 13, 1956				
17	150	333	198	224	-3.9	-3.8	+0.62
18							
19			79	114	-5.0	-4.7	+2.49
20			105	123	-6.2	-5.3	+0.09*
21			96	128	-6.0	-5.2	+2.94
22			114	119	-6.3	-5.8	+48.24*
23			136	180	-6.5	-5.7	+6.55
24			110	132	-8.5	-7.9	+34.06
			February 3, 1956				
13	33	125	189	198	-7.0	-6.5	+0.03*
14			246	255	-5.0	-4.9	+0.05
15			149	159	-4.0	-3.5	+0.03*
16			259	263	-1.0	-0.9	$\cong$0
17			263	286	-2.0	-1.5	+0.67
18			163	176	-4.5	-4.0	+0.12
19			237	263	-5.4	-4.9	+0.93
20			396	400	-4.1	-4.0	$\cong$0 *
21			404	427	-4.7	-4.6	+0.19
22			259	277	-5.2	-5.1	+0.15
23			211	216	-7.6	-7.5	$\cong$0 *
24			413	436	-6.6	-6.5	+0.19

*Values of u_* were negative for these computations.

Table 7. (Continued)

Time of Day	Z_1 cm	Z_2 cm	u_1 cm/sec	u_2 cm/sec	θ_1 °C	θ_2 °C	Q ly/hr
			February 28, 1956				
17	50	142	312	343	-10.9	-10.4	+1.91
18			237	268	-12.2	-11.8	+1.59
19			154	172	-15.3	-15.0	+0.53
20			145	159	-16.2	-15.3	+0.01*
21			154	228	-13.8	-13.5	+3.39
22			263	316	-13.8	-13.8	≃0
23			272	321	-12.6	-12.7	-0.76
24			356	378	-11.7	-12.0	-1.45
			March 1, 1956				
20	50	142	154	180	-4.2	-3.5	+1.84
21			128	154	-5.0	-4.5	+1.51
22			45	57	-9.5	-8.9	+0.01
23			136	159	-7.5	-6.9	+1.16
24			237	263	-5.0	-4.5	+1.51

E. CONDUCTION HEAT TRANSFER

1. SOIL HEAT TRANSFER

Heat is conducted from the warmer underlying ground to the snow cover. The flux of heat, although small when compared to daily amounts of heat transferred by radiation and convection, becomes significant when a complete snow season is considered. It is the result of thermal energy that is stored in the ground during the summer and early fall when no snow cover exists. More precisely, during the summer months, solar radiation heats the ground surface and establishes a temperature gradient directed into the ground. Heat is thus conducted into the ground as a function of both the magnitude of the temperature gradient and the conductivity of the ground itself. During the winter as the ground surface cools to 0°C or lower, the temperature gradient is reversed, causing heat to be conducted from the deeper warmer layers of the ground toward the snow-soil interface. If the ground is frozen to some depth before a permanent protective snow cover is deposited, a slow thawing of the ground occurs as heat is conducted upward from greater depths.

The flux of heat from ground to snow is proportional to the cross-sectional area of a plane parallel to the ground surface and to the temperature gradient in the direction of flow. If q is the flux of heat per unit area (in ly/sec), T the temperature, and Z the direction of the flow of heat,

$$q = - k\frac{\partial T}{\partial Z} \qquad (1)$$

The thermal conductivity, k, is an intrinsic property of the conducting substance For soils, the thermal conductivity is a function of the composition, density, and moisture content. However, although the heat flux by conduction is the result of both the temperature gradient and the thermal conductivity, an inverse relationship exists between them. In general, the greater thermal conductivity of the soil, the less the temperature gradient, since the better conduction tends to equalize temperature differences. Conversely, in a substance having a low thermal conductivity, such as snow, it is possible to maintain quite large temperature gradients.

Soil heat fluxes were measured by two Gier and Dunkle heat flow transducers (having built-in thermocouples) at 5 and 10 cm below the soil surface from 12 January 1955 through the remainder of one snow season. However, difficulties in recording heat flow measurements made it impossible to use the data as a basis for comparison with computed quantities. However, the consistency of the temperature difference between soil depths of 5 cm and 10cm between any two successive days suggested that one temperature difference per day could represent a meaningful average for that day. Table 8 lists the daily temperatures measured at 5 cm and 10 cm below the soil surface during the 1954-55 snow season. At 5 cm below the soil-snow interface the temperature ranged between +0.5°C and -0.9°C through the 1954-55 snow season. At the 10 cm depth, the range was between +0.9°C and -0.5°C. In January, February, and March the average temperature differences between 5 cm and 10 cm were 0.4°C, 0.2°C, and 0.1°C respectively. The decrease in temperature difference with time can be partially explained by the increase in the thermal conductivity of the soil as it became progressively more moist and partially by the gradual cooling of the soil to greater depths.

Daily quantities of soil heat flux were computed by means of equation (1). An appropriate soil thermal conductivity was difficult to select because of its dependence on soil composition, density, moisture content, and condition (frozen or unfrozen). Furthermore, soil composition and moisture content were not accurately known. Reference is made to Kersten (23) for an extensive tabulation of thermal conductivities of many different types of soils. Therefore, instead of rigidly applying one thermal conductivity, several were selected, and the conduction heat fluxes between 5 and 10 cm were computed for each. Table 9 summarizes the conductive heat fluxes between 5 cm and 10 cm as a function of thermal conductivity and temperature difference between the two depths. All heat fluxes in the table are directed upward.

Table 9

SOIL CONDUCTION HEAT TRANSFER (ly/day)

	k x 10^{-3} (cal cm^{-1} sec^{-1} deg^{-1})					
$T_{10cm}-T_{5cm}$ °C	1	2	3	4	5	6
.5	8.6	17.3	25.9	34.6	43.2	51.8
.4	6.9	13.8	20.7	27.6	34.6	41.5
.3	5.2	10.4	15.6	20.7	25.9	21.1
.2	3.5	6.9	10.4	13.8	17.3	20.7
.1	1.7	3.5	5.2	6.9	8.6	10.4

Based on soil density characteristics in the vicinity of the heat flow transducers, a thermal conductivity of 3.0 x 10^{-3} may be assumed. Assuming this value, heat flow quantities averaged about 21 ly/day in January, 10 ly/day in February, and 5 ly/day in March. These values compare to daily net radiation totals in January which range from a loss of about 90 ly/day with clear skies to a loss of about 5 ly/day with low overcast cloudiness and snow. In February, the values of net radiation with similar cloudiness conditions ranged from a loss of 80 ly/day to a gain of about 10 ly/day later in the month.

2. SNOW HEAT TRANSFER

The continuously changing thermal and physical properties of a snow cover and variations in heat transfer processes at its boundaries cause the theory of heat flow in snow to be much more complicated than that for homogeneous solids. The temperature wave in snow is complex, the liquid water content of snow varies with time and temperature, and the character of snow varies from layer to layer. The solution of heat transfer problems within the snow thus requires knowledge of depth and time changes in the thermal properties of snow, i.e., specific heat, conductivity, and diffusivity. For a snow cover whose conductivity does not vary with depth, a linear temperature profile indicates that inflow and outflow of heat for any layer are equal. A non-linear profile, on the other hand, indicates unequal inflow and outflow, with consequent changes in the temperature. The further assumption that there are no significant heat sources or sinks due to phase changes must be

made. Since conductivity is likely to vary with depth in a natural snow cover and since phase changes, although probably insignificant for short time intervals, are usually present, the foregoing principles can be applied only with qualification. Reference is made to work by Wilson (24) and Kondrat'eva (25) for detailed derivations of conduction heat transfer equations for a snow cover.

A method proposed by Liljequist (9) for computing conduction heat transfer quantities in snow was applied to the data obtained from daily snow pit observations. (Snow pit measurements are discussed in detail in a subsequent section.) The relative importance of the computations in the energy exchange of snow is difficult to evaluate quantitatively for two major reasons: (1) an accurate depth distribution of the variables (snow properties) which occur in the heat transfer equation for snow is difficult to measure and (2) one measurement of snow properties per day limits the validity of the computations only to the time of measurement. Small changes in snow properties exert pronounced effects upon conductive heat transfer. However, some insight into the complicated problem of conduction heat transfer in snow can be gained from the computations.

Based upon the development by Liljequist, the heat flux q(o) reaching the upper snow surface from below may be written:

$$q(o) = q(d) + L(o\text{-}d)$$

where q (d) = upward heat flux (ly/sec) at a reference level d. In the following computations d = 15 cm beneath the snow surface. L(o-d) = heat loss of the snow per unit time within a column with unit cross-section located between the surface and depth d. The flux q(d) may be computed from the equation

$$q(d) = k\left(\frac{\partial T}{\partial Z}\right)_d$$

The term $\left(\frac{\partial T}{\partial Z}\right)_d$ is the temperature gradient at the reference level d = 15cm, and k is the thermal conductivity of snow in gr cal cm^{-1} sec^{-1} deg^{-1}. The temperature gradient through the snow was interpolated from the temperature-depth curve measured once each day. The thermal conductivity of the snow was computed for each average snow density using a modified form of Abel's equation ($k = .0068\bar{\rho}^2$) proposed by Kondrat'eva (25): $k = .0085\bar{\rho}^2$, where $\bar{\rho}$ is average snow density in gm cm^{-3}.

To compute L(o-d), differences between the temperature measurements at the respective depths ($\Delta T = T_1 - T_2$) at the times t_1 and t_2 were determined. The loss of energy L(o-d) can then be written:

$$L(o\text{-}d) = \frac{c\,\rho_s}{t_2 - t_1} \int_o^d \Delta T\, dz$$

or

$$L(o\text{-}d) = \frac{c\,\rho_s\,d}{t_2 - t_1} \quad (\Delta T)m$$

where: c = specific heat of ice (0.5 cal/gm-deg)

$(\Delta T)m$ = average decrease or increase in temperature within the layer o-d, between successive snow profile observations (°C).

Quantities of snow conduction heat transfer were computed for 74 days in January, February and March of the two snow seasons and are given in Table 10. Values ranged from a heat gain of 17 ly/day to a loss of 35 ly/day. In the Antarctic, the highest loss observed by Liljequist was 0.038 ly/min, or about 55 ly/day.

Figure 7 illustrates a relationship between average air temperature and conduction heat transfer at the snow surface. Average air temperatures, listed in Table 11, are the means of temperatures measured at the adjacent weather station at 1400 EST and 2400 EST of the previous day and at the time of the snow profile observation. The gradual increase in heat losses with rapidly dropping average air temperatures reflects the low thermal conductivity of snow. The maximum loss occurred with an average air temperature of -13°C and a net radiation loss of about 90 langleys in the previous 24 hours. The maximum gain occurred with an average air temperature of -5°C and a net radiation loss of 30 langleys. In the latter example, the average temperature of the snow cover rose 9°C from the previous day resulting in a high L(o-d) term.

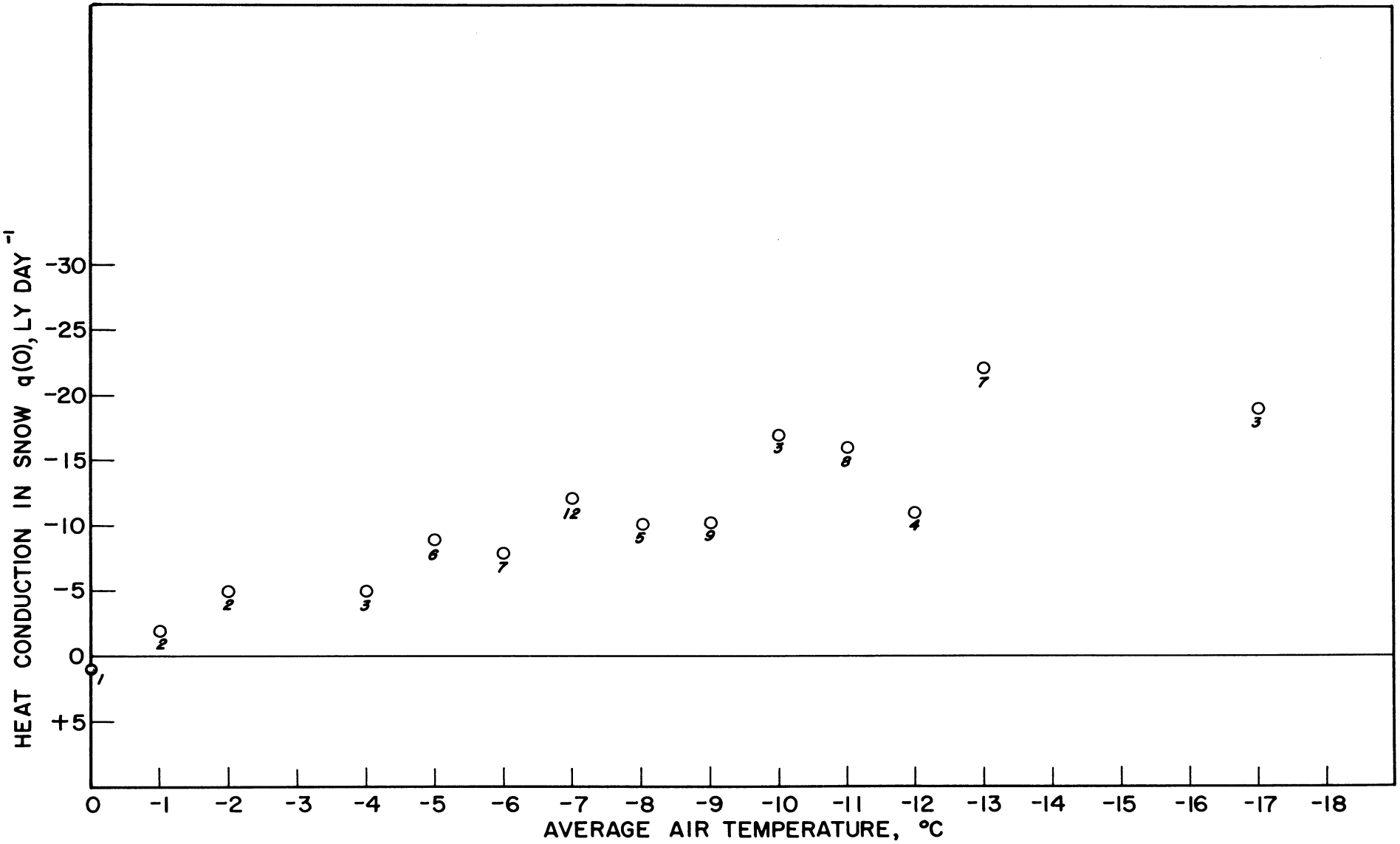

Fig. 7. Snow Heat Conduction versus Average Air Temperature of Previous 20 Hour Period. (The number of cases averaged for each point is indicated below it.) Negative quantities indicate heat lost.

Table 8

SOIL TEMPERATURE DATA
1955

Degrees Centigrade

Day of Month	January		February		March	
	5cm	10cm	5cm	10cm	5cm	10cm
1			+.1	+.5	-.4	-.1
2			-.1	+ 2	-.3	-.2
3			0	+.2	-.1	0
4			0	+.3	-.2	-.1
5			0	+.2	-.2	-.1
6					-.2	0
7			+.1	+.3	-.3	-.1
8			+.2	+.5	-.3	0
9			+.1	+.4	-.3	-.1
10			0	+.3	0	0
11			0	+.1	-.1	-.1
12			-.1	+.3	-.1	-.1
13	-.2	+.2	-.1	+.1	0	0
14	-.4	0	-.1	+.1	0	0
15	-.2	+.2	-.1	+.1	0	0
16	-.1	+.3	-.1	0	0	0
17	-.7	-.3	-.1	0	-.1	0
18	-.9	-.5	-.3	-.2	-.1	0
19	-.1	+.3	-.5	-.3		
20	-.1	+.3	-.2	-.1		
21	-.1	+.3	0	0		
22	0	+.4	0	0		
23	0	+.4	0	0		
24	0	+.4	+.1	+.2		
25	+.5	+.9	-.6	-.5		
26	+.3	+.7	-.5	-.2		
27	+.3	+.8	-.3	-.1		
28	+.5	+.9	-.4	-.1		
29	-.1	+.1				
30	-.1	-.5				
31	-.1	-.2				

Table 10

SNOW CONDUCTION HEAT TRANSFER DATA
Langleys/24 hr

Day of Month	1955			1956		
	Jan.	Feb.	Mar.	Jan.	Feb.	Mar.
1		-2.7	-7.9		-8.7	-3.3
2		-14.5	-3.6		-4.1	+0.2
3		-10.3	-6.2		-14.9	
4		-22.9	-4 6			
5	+1.6					
6	-20.2					+11.6
7	-29.6				-7.6	-16.6
8		-11.3			-4.2	-13.1
9		-0.4			-8.9	-20.4
10		-34.3	+0.8	+1.4	+4.7	
11	-7.8	-21.4	-17.7	-9.7		
12	-3.3			-33.4		
13	-12.0			-2.3		-14.2
14	-7.6				-8.6	-5.7
15		-8.5	-8.5		-6.0	-24.2
16		-3.8	-9.5		-10.8	-0.1
17		-33.3	-30.1	-13.4	-5.6	
18	-3.4	+10.1	-2.2	-6.4		
19	-6.9			-6.1		
20	-12.0			-7.1		+6.2
21					-6.0	+1.2
22					-14.9	+0.6
23					-35.4	-15.7
24		-21.5		-6.1	+17.5	
25	-5.9	-22.4		-8.0		
26	-9.2			-22.0		
27	-17.1			-15.6		
28	-14.5				-23.6	
29					-7.0	
30						
31				-5.5		

Table 11

FAA WEATHER STATION AIR TEMPERATURE DATA

Mean of air temperatures measured at 1400 EST and 2400 EST of previous day and 1000 EST of day indicated. Degrees Centigrade

Day of Month	1955 Jan.	1955 Feb.	1955 Mar.	1956 Jan.	1956 Feb.	1956 Mar.
1		-9	-5		-11	-4
2		-10	-6		-9	-1
3		-11	-7		-13	-4
4		-11	-6		-6	-8
5	-2	-5	-6		-5	-8
6	-6	-5	-11	-3	-2	-3
7	-9	-7	-16	-5	-4	-7
8	-3	-8	-15	-7	-1	-11
9	-6	-2	-1	-8	-4	-11
10	-9	-10	0	-5	-1	-7
11	-9	-17	-3	-5	-6	-8
12	-6	-16	-4	-7	-6	-12
13	-6	-16	-8	-4	-5	-11
14	-7	-9	-4	-5	-7	-7
15	-6	-12	-2	-2	-12	-12
16	-10	-6	-7	-3	-13	-9
17	-9	-13	-13	-7	-7	-4
18	-9	-3	-10	-6	-6	-5
19	-8	0		-5	-8	-5
20	-13	-1		-5	-9	-3
21	-5	-5		-18	-12	+2
22	-2	-10		-15	-11	-1
23	-6	-10		-8	-13	-7
24	-10	-11		-8	-5	
25	-9	-17		-9	-6	
26	-13	-5		-9	-12	
27	-17	-11		-7	-12	
28	-16	-8		-5	-13	
29	-16			-5	-7	
30	-16			-8		
31	-14			-9		

F. DIRECT RELATIONSHIPS

1. MEASUREMENT OF SNOW PROPERTIES

During the two snow seasons studied, several properties of snow were measured once daily at 1000 EST (except weekends) by digging a snow pit and sampling at different depths. The snow investigation site was part of a level horizontal testing field where the snow cover was deposited as uniformly as possible. However, because the snow depth, the character of the snow, and the temperature underwent changes at the point of excavation in the course of one day it was necessary to leave a certain distance between individual profile pits. It was thus impossible to eliminate the lateral heterogeneity of snow properties altogether, since the character of individual layers, or even that of the entire snow cover, could vary greatly between two snow pits in close proximity. Such variations are caused primarily by wind conditions during snow falls, small roughness of the ground, and slight undulations in the snow surface.

Snow properties which were considered to be of greatest importance to a study of the metamorphic process were density, temperature, and hardness. Temperatures were measured at 5cm increments through the snow. Density and hardness were measured at about 10cm increments. For the hardness data, a CNRC hardness gage was used which gave measures of resistance against horizontal penetration in gm/cm^2. Thus, it was possible to obtain a record of both the vertical density and hardness distributions and a more detailed record of the temperature distribution. From these measurements, time profiles were drawn which graphically presented the trends of snow properties with time, and enabled many individual results of a prolonged period of investigation to be compared and summarized. In addition, snow layers and the approximate crystal size within each layer were noted. In general, individual snow layers of different age were distinguished qualitatively by their grain size (fine, medium, coarse). Depth hoar was coarse-grained, very loose (cohesionless) snow, and crusts were snow layers that distinguished themselves from adjacent layers by their greater cohesiveness.

Depth hoar is the most coarse-grained type of snow that can form without the presence of the liquid phase. The conditions necessary for its formation are known, but the manner in which it is formed has not been completely explained. According to Bader (26), it has a porosity of 56 to 80%, a density between 30 to 40% and consists mostly of well-developed, hemimorphic crystals with a base, a prism, and pyramids. Complete cup formations are common. It has a preferred orientation. The basal planes are approximately parallel to the boundary of the snow layer, and the part terminated by pyramids is directed upward, which is the direction toward colder temperatures. The little cohesion that it usually possesses may almost become zero when its loose constituency is disturbed slightly. It possesses extreme properties, such as very large grain size, high air permeability, and low plasticity. It is never found at the surface of snow and occurs almost always near the ground. When under the influence of external pressure such as a heavy roller, this sugary textured snow acts much like dry sand and allows the roller to sink to the ground surface and actually "wash" a lateral wake of snow away from its path (27). One of the factors most conducive for depth hoar formation is air currents within the snow by means of which the deepest layers may suffer the loss of a large amount of material.

In natural snow, the transfer phenomenon is complicated by the simultaneous variation of many, if not all, external heat exchange processes which comprise the energy balance. Furthermore, within the snow itself, the absorption and transmission of heat vary with the character of the individual snow layers just as the structure, the liquid water content, density, porosity, and the temperature vary. Because of the interlocking complexities involving snow properties, time, and the various heat transfer processes, the problem of seeking a unique combination of meteorological parameters which accurately predict a snow property indicative of the metamorphic process is immense. It becomes necessary to combine snow properties into quantities more representative of the metamorphic process.

2. COLD CONTENT OF SNOW

Greater insight into the physical nature of a snow cover can be gained by evaluating its cold content, defined by the amount of heat required to warm the snow cover to 0°C (5). It represents the product $\bar{\rho} \times Z$ ($\bar{\rho}$ = mean density of a snow cover with a total depth Zcm), mean snow temperature $\bar{\theta}$, and specific heat c. Symbolically, the cold content of the entire layer Z_s is:

$$q = c \int_0^Z \rho_s \, \theta_s \, dZ \ (cal/cm^2)$$

where: c = specific heat of ice (0.5 cal/gm deg.)
ρ_s = density (gm/cm^3)
θ_s = snow temperature at a depth Z (°C)

Quantities of cold content were computed using data from each snow pit observation for both snow seasons and are listed in Table 12. Day to day changes in the average temperature of the snow cover were generally the most pronounced influences on cold content variations. Net radiation and mean air temperatures seemed to be its possible predictors. Algebraic sums of hourly totals of net radiation for the 24 hour period ending at the times of snow pit observations were computed. Average air temperatures are identical to those computed for the snow heat conduction analysis. Both predictors were tested independently and also simultaneously. Poor correlation resulted by relating only net radiation totals to cold content. Apparently significant correlation, on the other hand, resulted by relating mean air temperatures to cold content. Results are shown in Figure 8. A combination of the two predictors graphed against cold content did not improve the correlation. The cold content reached its greatest negative value of 42.8 cal cm^{-2} on 25 February, 1955, when the mean air temperature was -17°C, the 24 hour net radiation total was -13 langleys, the snow depth was 37cm, and the average snow density was 0.26 g/cm^3. This was the result of a fair weather period accompanied by the influx of extremely cold air. The temperature profile through the snow between 5cm above ground and 5cm below the snow surface in the example was 13°C.

3. VERTICAL TEMPERATURE GRADIENT IN SNOW AND ITS EFFECTS

The magnitude of the temperature difference between the warm ground and the colder snow cover is, above all, decisive for the ensuing metamorphism into angular grained, coarse crystalline snow and finally into the hollow forms of depth hoar (26). A necessary condition for the formation of depth hoar through metamorphism is sufficient air permeability of the snow. Moist air fills the voids in the snow and begins to circulate at the slightest

difference in temperature. Air movement primarily regulates not only temperatures in the snow but also transports the water vapor that is absorbed or given off by the ice crystals during temperature changes. The air enclosed within the freshly fallen crystals of new snow is estimated to represent far less than 1% of the total volume of the voids. Within a few days the communication among voids is almost complete, and remains so up to very high densities. By diffusion and convection, vapor flows from the deeper, warmer snow layers to the higher colder layers where it condenses because of its supersaturation. Also, because of the non-linear relationship between vapor pressure and temperature, the most intensive changes are produced in the warmest layers, i.e., those nearest the ground. The individual orientation of crystals with respect to the vapor flow and their local temperature conditions affect the growth selection by the individual crystals, since the temperature gradient is not a smooth curve in the range of grain dimensions. The layers which are transformed the most are those which are deposited loosely and are able to maintain their air permeability during metamorphism.

As a result of the transfer process, the vapor lost from the lower layers will be compensated by a spontaneous conversion of snow from the solid to a gaseous phase, i.e., vaporization of the snow particles without their conversion into a liquid phase and subsequent evaporation. In this manner, after a time, the lower layers of the snow cover undergo some disintegration and the upper layers become denser.

Laboratory studies with fresh snow were conducted by deQuervain (28) to determine how certain properties of snow change with time when kept under various conditions of pressure and temperature. He found that in the absence of a temperature gradient, fresh snow is transformed into a fine granular material whose hardness and strength as well as specific gravity increase considerably with a rise of temperature and load. On the other hand, in the presence of a temperature gradient, fresh snow is transformed into the coarse granular material of depth hoar. The greater the temperature difference between the cold snow surface and the warmer ground below, the more intense will the internal transfer be and the sooner will the transformation to depth hoar occur. Kondrateva (7) showed that with a temperature gradient of 11°C, the density of the lower layer decreased by 0.08 gm cm^{-3} in 5 days using a depth of 45cm of artifically compacted snow to attain density variation.

The snow temperature profile and its dependence on external energy exchange processes were studied for both snow seasons. Net radiation and mean air temperature were related to the temperature profile, but the most consistent estimates of the magnitude of the temperature gradient through the snow resulted by relating average air temperatures, as in the snow heat conduction analysis, to the temperature profile from 5cm below the snow surface to 5cm above ground, shown in Figure 9. Temperature gradients between the two snow depths ranged from 15°C with a mean air temperature of -13°C and a net radiation loss of about 90 langleys in the previous 24 hour period, to less than 1°C with a mean air temperature of +2°C late in a snow season. Radiation measurements were not available in the latter example.

4. SNOW HARDNESS

Because of the importance of snow depth, density, and hardness to the development of a trafficable surface and their effects on the loadbearing capacity of a snow cover, the inter-relationships of these properties were investigated. Hardening is a metamorphic process which causes marked changes in the mechanical properties of snow independent of those produced only by a

change in density. It is defined by the resistance of a material to penetration by another material without undergoing permanent deformation. In the hardening process, the individual snow crystals or grains become bonded to each other by ice bridges.

Hardness measurements were graphed against snow depth and density for both snow seasons. Figure 10 is a composite of all data. Snow depths for all values exceeded 30cm. The isolines of hardness were terminated because of lack of adequate data. In general, hardness increased with density and depth except in the cases where depth hoar was observed in the lower layers. However, the coarse-grained deep layers were subjected to the pressure induced by the weight of upper snow layers and a greater penetration resistance could in many cases be attributed to their resulting greater incompressibility, not necessarily to a greater strength. Pure depth hoar, however, had an extremely low penetration resistance and was responsible for some anomalies in the hardness pattern.

The strength characteristics of depth hoar corresponded closely to those observed by Haefeli at Weissflujoch (29), in that the slightest mechanical disturbance brought about a sudden change in structure and density, causing the delicate crystalline conglomerate to crumble like a house of cards and to approach a state of maximum consolidation, in a matter of hours. Such agitation creates a state of physical instability for the countless new points of contact among the snow particles which comprise the snow cover. As equilibrium is gradually reestablished, coalescence of many of these contact points results, and the aggregate of the recrystallized bonds reinforces the original hardness of the snow cover. Taylor (27) discusses a harrowing process to pulverize and agitate particles of snow comprising a deep snow cover which built up densities exceeding 0.60 gm/cm^3. He points out that by processing snow at higher temperatures, such as in the afternoon, advantage may be taken of the rapidly falling air temperatures to enable increased hardness through greater ice bonding, thus making maximum use of the effects of density and temperature on hardness and supporting capacity of snow.

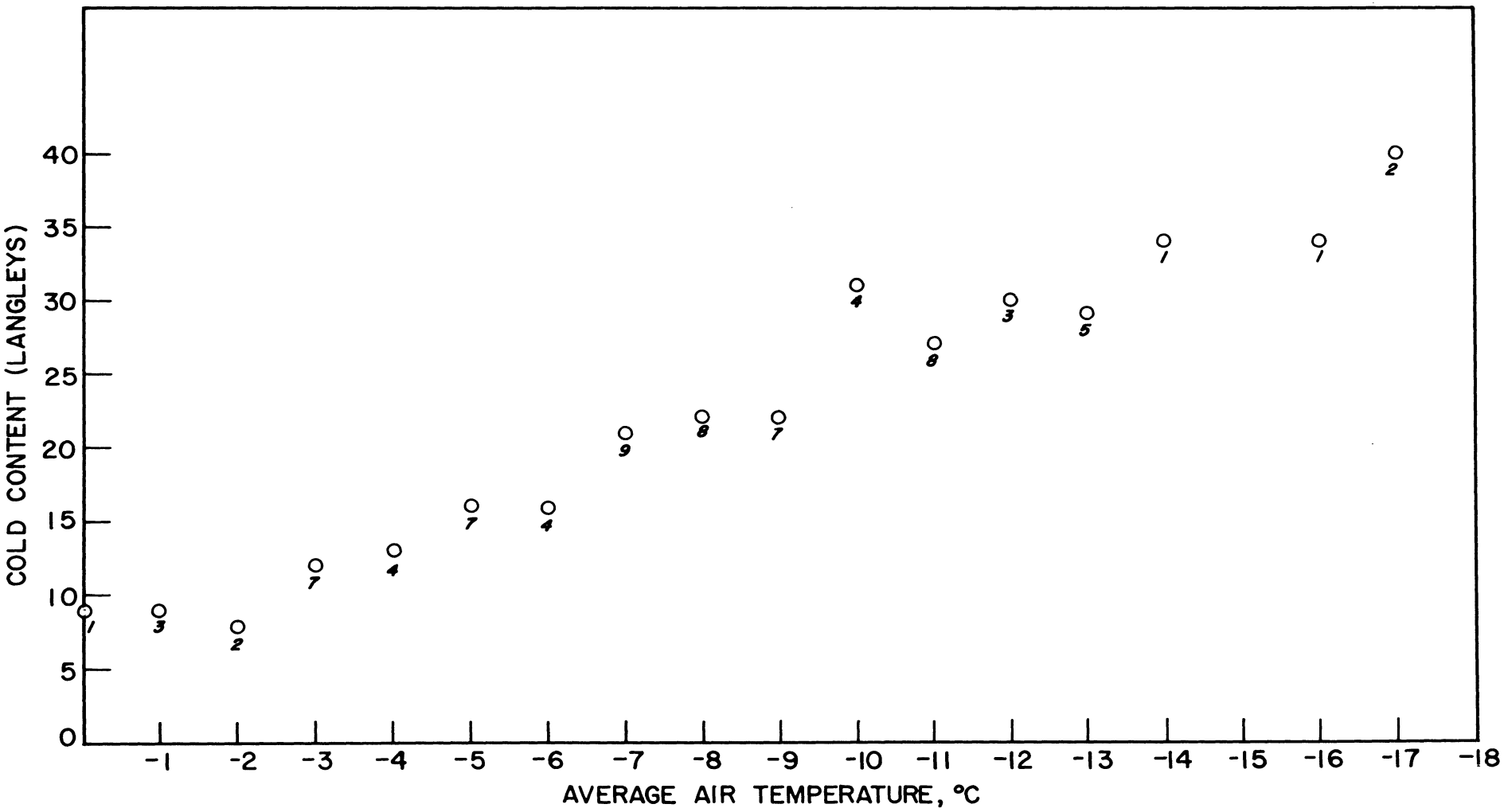

Fig. 8. Snow Cold Content versus Average Air Temperature of Previous 20 Hour Period. (The number of cases averaged for each point is indicated below it.)

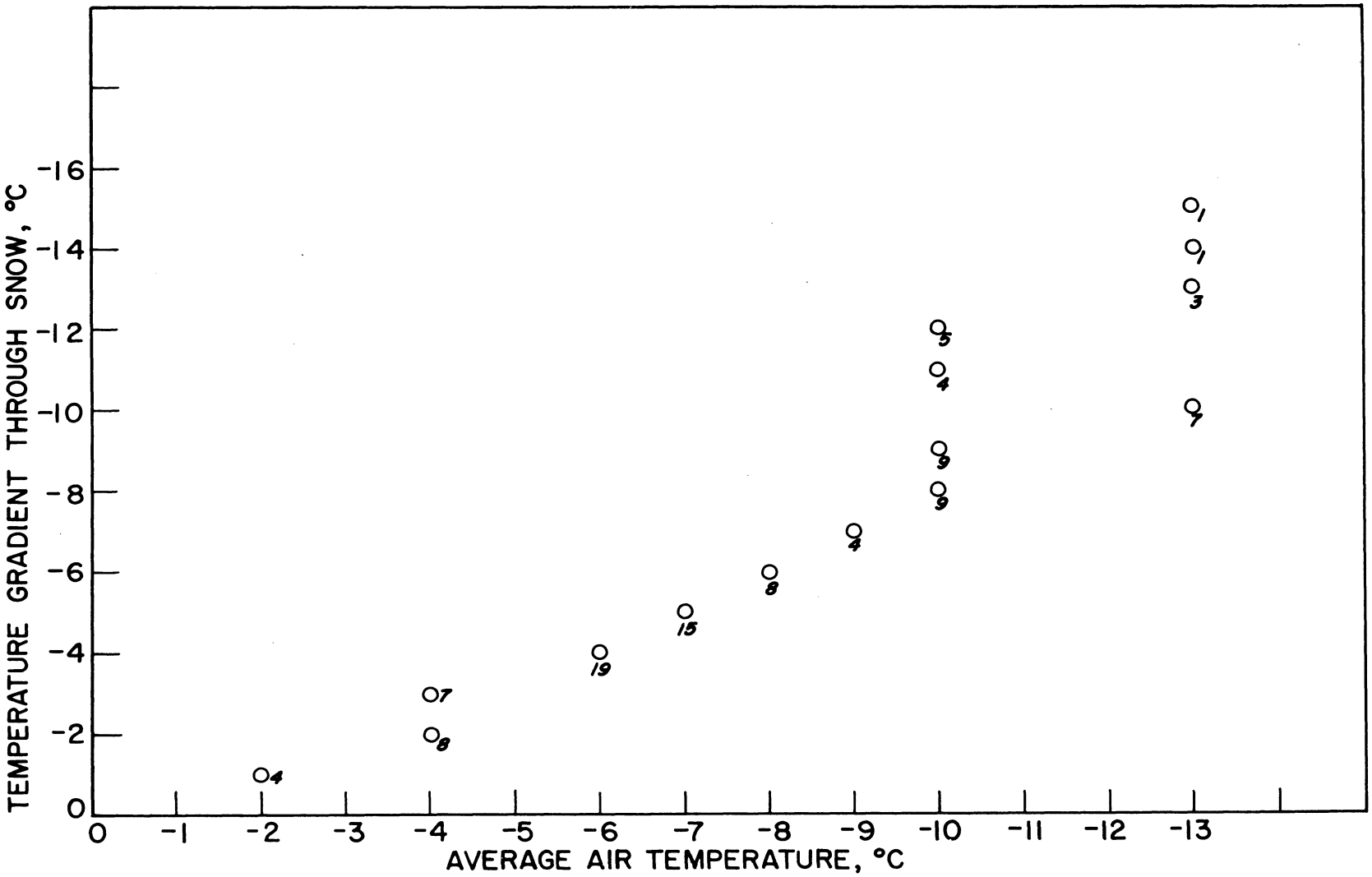

Fig. 9. Snow Temperature Difference Between 5cm Below the Snow Surface and 5cm above Ground versus Average Air Temperature of Previous 20 Hour Period. (The number of cases averaged for each point is indicated below it.)

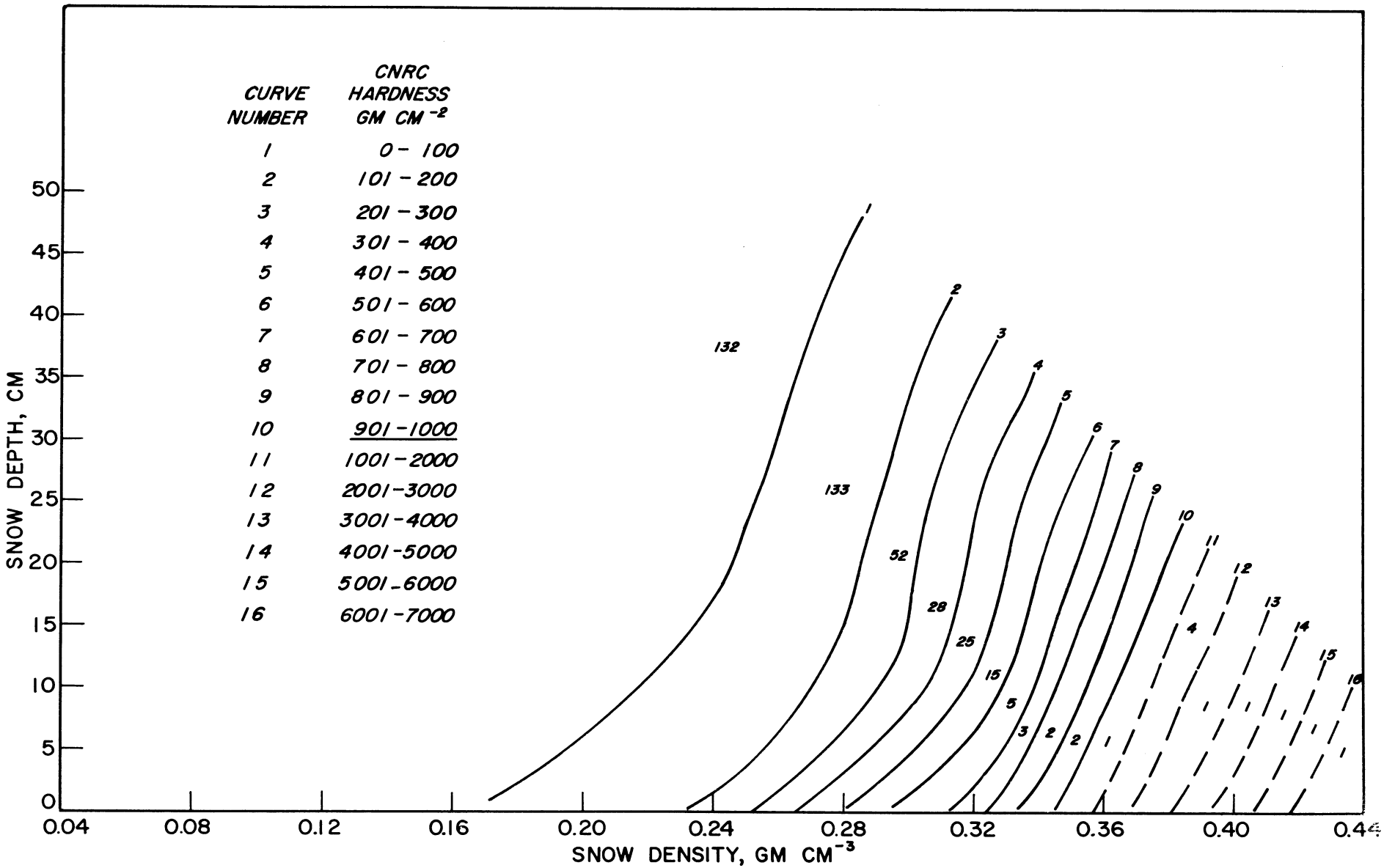

Fig. 10. Snow Hardness versus Depth and Density. (The number of cases is indicated in the region of greatest concentration.)

Table 12

SNOW COLD CONTENT DATA
Langleys

Day of Month	1955			1956		
	Jan.	Feb.	Mar.	Jan.	Feb.	Mar.
1		18.7	17.6		16.9	11.3
2		27.6	15.5		14.5	9.3
3		20.7	14.9		30.2	
4		36.6	14.4			
5	0					22.3
6	4.8			13.3	8.3	11.0
7	11.0	17.7	33.7		13.2	21.1
8		17.7			8.6	21.4
9		8.1	10.4	28.9	11.7	32.1
10	7.7	29.8	8.8	15.4	5.6	
11	6.6	38.0	12.1	12.5		
12	3.3			28.6		22.9
13	3.6			18.2	27.7	27.7
14	5.7	41.8	9.6		20.8	30.0
15		34.5	7.8		16.1	34.9
16		18.7	21.3	10.3	24.3	22.7
17	6.7	33.3	32.9	15.6	16.3	
18	6.4	15.5	38.5	16.3		
19	8.9			13.6		26.6
20	13.0			10.8	9.7	11.4
21		20.4			14.3	10.9
22					20.5	6.9
23		28.6		28.2	32.9	12.5
24	11.7	24.1		15.6	9.8	
25	13.7	42.8		16.8		
26	18.4			20.5		
27	28.2			24.8	22.6	
28	32.6	21.9			25.0	
29					23.3	
30				18.5		
31	33.8			20.1		

G. SUMMARY AND CONCLUSIONS

1. THERMAL RADIATIVE HEAT TRANSFER

a) The per cent of daily incident solar radiation at the outer limit of the earth's atmosphere which reaches the snow surface, when related to cloudiness, ranged from 94 with clear skies to less than 20 with an overcast less than 1000 feet high with precipitation. Average diurnal patterns of total solar radiation may be estimated for various cloudiness. Total solar radiation measured with overcast clouds less than 5000 feet high averaged about 70% of the clear-sky radiation.

b) Values of atmospheric radiation were related to instrument shelter temperatures during clear nights. The resulting curve paralleled the black body radiation curve, although about 7 ly/hr lower in absolute values.

c) Atmospheric radiation during clear skies was about 9 ly/hr less than that with low overcast conditions with no snow falling. In the presence of falling snow, values of total hemispherical radiation were about 5 ly/hr greater than with no snow falling but with similar low overcast cloudiness.

d) With low overcast cloudiness, the net longwave exchange averaged about -17 ly/day in January and -8 ly/day in February. With clear skies the net longwave exchange averaged about -128 ly/day in January and -120 ly/day in February.

e) The net radiation exchange with clear skies during midday in January remained slightly negative and became increasingly positive through February. The highest positive values of net radiation occurred during the daytime with low overcast or broken cloudiness and precipitation. The largest net radiational loss of 9 ly/hr occurred at night with clear skies and nearly calm winds.

2. CONVECTIVE HEAT TRANSFER

a) The average magnitude of surface temperature inversions over snow was related to weather station observations of cloudiness and wind speeds for both day and night. With winds of 12 knots or greater, the temperature difference in the first 10 meters was usually near adiabatic even with clear skies at night. During the day, inversions seldom exceeded 1-2°C, and a slight lapse commonly occurred during low overcast conditions and moderate winds.

b) The Liljequist model of turbulent heat transfer more adequately describes turbulent transfer processes over snow than does that of Monin and Obukhov. Average heat transfer quantities were related to cloudiness and wind speed measurements.

3. HEAT TRANSFER PROCESSES IN SOIL AND SNOW

a) The accuracy of the computations of conduction heat transfer in soil could not be ascertained because of the lack of adequate data from which soil thermal conductivity could be estimated.

b) Computations of conduction heat transfer in snow employing the Liljequist method showed significant correlation with average air temperatures.

c) Average values of snow cold content can be estimated from average air temperatures. Net radiation, when used as an additional predictor of cold content, did not significantly improve the correlation.

d) Average temperature differences through the snow, responsible for metamorphic action leading to the formation of depth hoar, could be estimated by a knowledge of the previous 20 hour average temperature.

e) Snow hardness distributions, indicators of the supporting capacity of snow, could be estimated graphically from snow density and depth observations

PART III

PARTICIPATION IN DATA COLLECTION PROGRAM

1. FIELD TEST, JANUARY, 1958

A special field test of wind and temperature profile measurement systems was conducted at the Keweenaw Field Station during the last week of January, 1958. The University of Michigan profile measuring equipment was operated alongside the SIPRE field equipment to enable data comparison. It consisted of a four meter mast upon which were mounted four Beckman and Whitley cup anemometers and four number 36 B. and S. gauge copper-constantan thermocouples junctions mounted in flat plate radiation shields. Sensor levels were at 0.5, 1.0, 2.0, and 4.0 meters above the snow surface. The SIPRE field equipment consisted of both Friez and Instruments Corporation of America cup anemometers and shielded, and aspirated, copper constantan thermocouple junctions.

The data obtained with the University of Michigan measurement system consisted of 62 fifteen minute wind profiles supplemented by 20 temperature profiles. A comparison of the two sets of data revealed discrepancies in average temperature as well as unexplained fluctuations in temperatures recorded and printed by the SIPRE digital printout system. This information and remedial suggestions were forwarded to director, Climatic and Environmental Research Branch, on 25 February 1958.

The radiation data obtained during the tests were evaluated by comparing computed values of various terms of the radiation balance with measured values. Good agreement resulted. Similarly, the integrator of the digital converter system was investigated for accuracy by comparing 15 minute integral values obtained from the digital printout system with those obtained from the recorder chart by visual-manual integration.

The wind profiles obtained by both SIPRE and the University of Michigan anemometers were graphed on semi-log paper. The relative accuracy of the two systems was determined by considering the slopes of the profiles. Their absolute accuracy was determined by considering the intercepts on the height ordinate. Because profile curvature during non-adiabatic conditions prevented profile comparison and identification, both comparisons were determined only during adiabatic conditions. In general, identical slopes were obtained for wind speeds between 5 mph and 15 mph. However, the intercepts were different in almost every case, which resulted in different surface roughness values. A comparison of two SIPRE and one Beckman and Whitley anemometer mounted on a horizontal bar and exposed to an average natural wind of 16 mph disclosed that a multiplying factor of 1.017 and 1.036, respectively applied to each SIPRE anemometer would bring them into agreement with the Beckman and Whitley system.

2. PARTICIPATION IN 1958-59 SNOW SEASON PROGRAM

Based upon preliminary data analyses, and a pre-season check-out of sensor and system performance in October, 1958, a list of comments and suggestions for improved operation of the Keweenaw Field Station data collection system for the 1958-59 snow season was formulated. The suggestions

pertained mainly to modification in measurement procedures in order to improve sensor accuracy and recording resolution. The list was submitted to the director, Climatic and Environmental Research Branch, and approval was granted not only to implement several minor modifications but also to obtain special sets of data for detailed analysis. As a result, University of Michigan personnel began participation in the Keweenaw Field Station data collection program on November 24, 1958. During the initial three weeks, considerable effort was directed toward calibrating various recorders, testing sensors, eliminating spurious indications, improving sensor exposures, and improving recording resolution. Also, field testing of the newly installed visibility attenuation meter was initiated.

The data collection system was operated continuously through the 1958-59 snow season except for brief periods during which individual components were tested or modified or during which there were equipment failures. Special effort was devoted to data analysis, recorder calibration, Dewcel and anemometer testing and matching, and snow surface temperature measurement. Detailed sets of data were obtained on several days when steady snowless weather conditions prevailed. During these periods, the data logging system was operated at five minute intervals, snow surface temperatures were measured, and all recorders and sensors were ascertained to be functioning at their greatest possible accuracy. In addition, snow pit observations were initiated early in December and continued throughout the snow season, which happened to be a near record in total snowfall.

REFERENCES

1. Gerdel, R. W., M. Diamond, and K. J. Walsh, "Nomographs for Computation of Radiation Heat Supply", SIPRE Research Paper 8, 6pp., February, 1954.

2. Klein, W. H., "Calculation of Solar Radiation and the Solar Heat Load on Man", Journal of Meteorology, Vol. 5, No. 4, pp. 119-129, August, 1948.

3. Elsasser, W. M., "Heat Transfer by Infrared Radiation in the Atmosphere", Harvard Meteorological Studies, No. 6, 107 pp., 1942.

4. Brooks, D. L., "A Tabular Method for the Computation of Temperature Change by Infrared Radiation in the Free Atmosphere", Journal of Meteorology, Vol. 7, No. 5, pp. 313-321, October, 1950.

5. Eckel, O. and C. Thams, "Investigations on Conditions of Density, Temperature, and Radiation of the Davos Snow Cover" (Untersuchungen über Dichte-Temperatur und Strahlungsverhältnisse der Schneedecke in Davos), Snow and its Metamorphism (Der Schnee und seine Metamorphose) by H. Bader and others. Beitrage zur Geologie der Schwiez, Geotechnische Serie, Hydrologie, Lieferung 3, 1939, SIPRE Translation 14, pp. 245-303, 1954.

6. Monin, A. S., and A. M. Obukhov, "Basic Laws of Turbulent Mixing in the Ground Layer of the Atmosphere", (Osnovnye Zakonomernosti Turbulentnogo Peremeshwaniia v Prizemnom Sloe Atmosfery), Akademiia Nauk SSSR, Leningrad, Geofizicheskii Institut, Trudy, Vol. 151, No. 24, pp. 163-187, 1954.

7. Sheppard, P. A., "Transfer Across the Earth's Surface and Through the Air Above", Quarterly Journal of the Royal Meteorological Society, Vol. 84, No. 361, pp. 205-224, July, 1958.

8. Sverdrup, H. U., "The Eddy Conductivity of the Air Over a Smooth Surface", Geofysiske Publkasjoner, Vol. 11, No. 7, 49pp., Oslo, 1936.

9. Liljequist, G. H., "Wind Structure in the Low Layer", Energy Exchange of an Antarctic Snow Field, Norwegian-British-Swedish Antarctic Expedition Scientific Results, Vol. 2, Part 1C, pp. 188-234, Oslo, 1957.

10. Liljequist, G. H., "Surface Inversions and Turbulent Heat Transfer", Energy Exchange of an Antarctic Snow Field, Norwegian-British-Swedish Antarctic Expedition Scientific Results, Vol. 2, Part 1D, pp. 237-274, Oslo, 1957.

11. Halstead, M. H., R. L. Richman, W. Covey and J. D. Merryman, "A Preliminary Report on the Design of a Computer for Micrometeorology", Journal of Meteorology, Vol. 14, No. 4, pp. 308-325, August, 1957.

12. Poppendiek, H. F. and M. Tribus, "A Comparison of Several Heat and Mass Transfer Networks of Interest in Water Conservation", Transactions, American Geophysical Union, Vol. 32, No. 1, pp. 49-56, February, 1951.

13. Merryman, J. D., and W. Clayton, "A Dynamic Wind Simulator for the Frictional Boundary Layer", Journal of Meteorology, Vol. 16, No. 2, pp. 155-166, April, 1959.

14. Clayton, W. H., W. G. Covey and J. D. Merryman, Design of Experimental Meteorological Simulators, The A. and M. College of Texas, 109pp., January, 1959.

15. Budyko, M. I., "The Heat Balance of the Earth's Surface", (Teplovoi Balans Zemnoi Poverknosti), Gidrometeorologicheskoe Izdatel'stvo, Leningrad, 1956, U. S. Department of Commerce Translation, 255pp, 1958.

16. Corps of Engineers, U. S. Army, "Melting of the Snowpack", Snow Hydrology, pp. 141-186, June, 1956.

17. Diamond, M. and R. W. Gerdel, "Radiation Measurements on the Greenland Ice Cap", SIPRE Research Report 19, 21pp., October, 1956.

18. Hoeck, E., "Influence of Radiation and Temperature on the Melting Process of the Snow Cover", (Der Einfluss der Strahlung und der Temperatur auf den Schmelzprozess der Schneedecke), Beitrage zur Geologie der Schweiz, Geotechnische Serie Hydrologie, Leiferung 8, pp. 1-36, 1952, SIPRE Translation 49, January, 1958.

19. Liljequist, G. H., "Short-wave Radiation", Energy Exchange of an Antarctic Snow Field, Norwegian-British-Swedish Antarctic Expedition Scientific Results, Vol. 2, Part 1, pp. 1-109, Oslo, 1956.

20. Liljequist, G. H., "Long-wave Radiation and Radiation Balance", Energy Exchange of an Antarctic Snow Field, Norwegian-British-Swedish Antarctic Expedition, Scientific Results, Vol. 2, Part 1B, pp. 116-183, Oslo, 1956.

21. Priestley, C. H. B., "A Determinant Hypothesis for the Superadiabatic Wind and Temperature Profiles", Quarterly Journal of the Royal Meteorological Society, Vol. 86, No. 368, pp. 232-236, April, 1960.

22. Ellison, T. H., "Turbulent Transport of Heat and Momentum from an Infinite Rough Plane", Journal of Fluid Mechanics, Vol. 2, Part 5, pp. 456-466, July, 1957.

23. Kersten, M. S., Thermal Conductivity of Soils, Bulletin of the University of Minnesota Institute of Technology, Vol. L11, No. 21, June, 1949.

24. Wilson, W. T., "An Outline of the Thermodynamics of Snowmelt", Transactions of the American Geophysical Union, pp. 182-195, June, 1941.

25. Kondrat'eva, A. S., "Thermal Conductivity of the Snow Cover and Physical Processes Caused by the Temperature Gradient" (Teploprovodnost Snegovogo Pokrova i Fizicheskie Protsessy, Proiskhodiaschie v Nem pod Vlianiem Tempuraturnogo Gradienta), Physical and Mechanical Properties of Snow and Their Utilization in Airfield and Road Construction, Moscow-Leningrad: Academiia Nauk SSSR, pp. 14-28, 1945, SIPRE Translation 22, March, 1954.

26. Bader, H., "Mineralogical and Structural Characterization of Snow and its Metamorphism", Snow and its Metamorphism (Der Schnee und seine Metamorphose) by H. Bader and others, Beitrage zur Geologie der Schwiez, Geotechnische Serie, Hydrologie, Lieferung 3, 1939, SIPRE Translation 14, pp. 5-55, 1954.

27. Taylor, Major A., Snow Compaction, SIPRE Report 13, 63pp., January, 1953.

28. deQuervain, M. R., "On Metamorphism and Hardening of Snow Under Constant Pressure and Temperature Gradient", Extract des Comptes Rendus et Rapports, Tome IV, p. 225-239, 1957.